# Perspectives for regulating 10 nm particle number emissions based on novel measurement methodologies

Z. Samaras, M. Rieker, E. Papaioannou, W.F. van Dorp, M. Kousoulidou, L. Ntziachristos, J. Andersson, A. Bergmann, S. Hausberger, J. Keskinen, et al.

# Perspectives for regulating 10 nm particle number emissions based on novel measurement methodologies

*Authors:*

Z. Samaras[1], M. Rieker[2], E. Papaioannou[3], W.F. van Dorp[4], M. Kousoulidou[5], L. Ntziachristos[1], J. Andersson[6], A. Bergmann[7], S. Hausberger[8], J. Keskinen[9], P. Karjalainen[9], S. Martikainen[9], A. Mamakos[10], Ch. Haisch[11], A. Kontses[1], Z. Toumasatos[1], L. Landl[8], M. Bainschab[7], T. Lähde[23], O. Piacenza[13], P. Kreutziger[2], A. N. Bhave[14], K. F. Lee[14], J. Akroyd[15,16], M. Kraft[15,16,17], M. Kazemimanesh[18], A.M. Boies[18], C. Focsa[19], D. Duca[19], Y. Carpentier[19], C. Pirim[19], J. A. Noble[19,20], O. Lancry[20], S. Legendre[20], T. Tritscher[21], J. Spielvogel[21], H.G. Horn[21,†], A. Pérez[22], S. Paz[22], D. Zarvalis[3], A. Melas[23], P. Baltzopoulou[3], N. D. Vlachos[3], L. Chasapidis[3], D. Deloglou[3], E. Daskalos[3], A. Tsakis[3], A. G. Konstandopoulos[3,24], S. Zinola[25], S. Di Iorio[26], F. Catapano[26], B. M. Vaglieco[26], H. Burtscher[27], G. Nicol[13], D. Zamora[29] and M. Maggiore[30]

[1] *Aristotle University, Lab of Applied Thermodynamics, GR-54124 Thessaloniki, Greece*

[2] *HORIBA Europe GmbH, Hans-Mess-Str. 6, 61440 Oberursel, Germany*

[3] *Centre for Research and Technology-Hellas (CERTH), 6th km Charilaou-Thermi, 57001 Thermi, Greece*

[4] *Uniresearch B.V., Delftechpark 37j, 2628 XJ Delft, Netherlands*

[5] *European Climate, Infrastructure and Environment Executive Agency, European Commission, Brussels, Belgium*

[6] *Ricardo Automotive & Industrial, Shoreham Technical Centre, Shoreham by Sea, BN43 5FG, England*

[7] *University of Technology Graz, Institute of Electronic Sensor Systems, Inffeldgasse 19, A-8010 Graz, Austria*

[8] *University of Technology Graz, Institute for Internal Combustion Engines and Thermodynamics, Inffeldgasse 10/II, A-8010 Graz, Austria*

[9] *Tampere University, Aerosol Physics Laboratory, PL 692, FIN-33014 Tampere, Finland*

[10] *AVL List GmbH, Hans-List-Platz 1, 8020 Graz, Austria*

[11] *Technical University of Munich, Institute of Hydrochemistry and Chair for Analytical Chemistry, Marchioninistr. 17, D-81377 München*

[13] *Centro Ricerche Fiat, 10043 Orbassano, Italy*

[14] *CMCL Innovations, Castle Park, Cambridge, CB3 0AX, United Kingdom*

[15] *Department of Chemical Engineering and Biotechnology, University of Cambridge, United Kingdom*

[16] *CARES, Cambridge Centre for Advanced, Research and Education in Singapore, 1 Create Way, CREATE Tower, #05-05, Singapore, 138602*

[17] *School of Chemical and Biomedical Engineering, Nanyang Technological University, 62 Nanyang Drive, Singapore, 637459*

[18] *University of Cambridge, Department of Engineering, Cambridge, United Kingdom, CB2 1PZ*

[19] *Univ. Lille, CNRS, UMR 8523 - PhLAM - Physique des Lasers, Atomes et Molécules, Lille F-59000, France*

[20] *Horiba Scientific, HORIBA France SAS, Palaiseau, France*

[21] *TSI GmbH, Neuköllner Str. 4, 52068 Aachen, Germany*

[22] *IDIADA Automotive Technology SA, L'Albornar E-43710, Santa Oliva (Tarragona), Spain*

[23] *European Commission, Joint Research Centre (JRC), 21027 Ispra, Italy*

[24] *Department of Chemical Engineering, Aristotle University Thessaloniki, P.O. Box 1517, 54006 Thessaloniki, Greece*

[25] *IFP Energies nouvelles, Rond-point de l'échangeur de Solaize, BP 3, 69360 Solaize, France ; Institut Carnot IFPEN Transports Energie*

[26] *Istituto di Scienze e Tecnologie per l'Energia e la Mobilit`a Sostenibili STEMS – CNR, 80125, Naples, Italy*

[27] *Institute for Aerosol and Sensor Technology, Fachhochschule Nordwestschweiz, 5210 Windisch, Switzerland*

[28] *Centro Ricerche Fiat, 10043 Orbassano, Italy*

[29] *Mobility Ion Technologies SL (MION) , C. Juncal 3, 47195, Valladolid, Spain*

[30] *Directorate General for Research and Innovation, European Commission, Brussels, Belgium*

[†] *Deceased.*

Contact details:

| ***DownToTen*** | ***PEMs4Nano*** | ***SUREAL-23*** |
|---|---|---|
| Coordinator: Prof. Dr Zissis Samaras | Coordinator: Prof. Dr Marcus Rieker | Coordinator: Dr Eleni Papaioannou |
| Lab of Applied Thermodynamics | HORIBA Europe GmbH | Aerosol & Particle Technology |
| Dept of Mechanical Engineering | Hans Mess Str. 6 | Laboratory CERTH/CPERI |

| | | |
|---|---|---|
| Aristotle University<br>54124 Thessaloniki, Greece<br>zisis@auth.gr<br>http://www.downtoten.com/ | D-61440 Oberursel<br>marcus.rieker@horiba.com<br>http://pems4nano.eu/ | PO Box 60361, 6th km Charilaou-Thermi Rd<br>Thessaloniki 57001, Greece<br>helen@cperi.certh.gr<br>http://sureal-23.cperi.certh.gr/ |


| | | |
|---|---|---|
| Funded under H2020 Grant Agreement: 724085 | Funded under H2020 Grant Agreement: 724145 | Funded under H2020 Grant Agreement: 724136 |



## Keywords (1-6)

Particulate matter, particle number, particle emissions measurements, sub-23 nm particles, internal combustion engines, measurement procedures

## Abstract

Concerns regarding noxious emissions from internal combustion engines have increased over the years. There is a strong need to understand the nature of sub-23 nm particles and to develop measurement techniques to evaluate the feasibility of new regulations for particle number emissions in the sub-23 nm region (down to at least 10 nm).

This paper presents the results of three EU-funded projects (DownToTen, PEMs4Nano and SUREAL-23) which supported the understanding, measurement and regulation of particle emissions below 23 nm and have successfully developed sub-23 nm particle measurement devices, specifically laboratory systems and mobile devices for RDE tests. The new technology was validated in chassis dyno tests and on the real road. The results show that sub-23 nm particles are mainly generated at the engine start and during acceleration phases. The innovations show that the technology is mature and robust enough to serve as a basis for regulating sub-23 nm particles.

# 1. Introduction

## *1.1. Intro: air quality and existing regulations*

The EU air quality in general is steadily improving. However, in many major European cities and globally it still remains problematic, in particular concerning $NO_2$ and particulate emissions. Road traffic contributes significantly to particle number (PN) concentrations and can reach 90% in busy roads (Kumar et al., 2010). Currently, there is no PN air qulatity standard and regulation relies only on precautionary measures such as limitng the emount of vehicle emisisons. The EU emissions regulation requires that the solid particle number for particles larger than 23 nm (SPN23) is measured for type approval of diesel and gasoline direct injection (GDI) light-duty vehicles, since 2011 (Euro 5b) and 2014 (Euro 6), respectively. For diesel light-duty vehicles and for GDI LDVs, the limit is $6\times10^{11}$ particles/km under Regulations 692/2008 and 459/2012 respectively. These limits need to be respected on the road with the real-driving emissions (RDE) regulation. Also, testing on the road with portable emissions measurement systems (PEMS) for SPN23 and $NO_x$ during type approval (Regulation 2016/427) and in-service conformity (RDE 4th package) were introduced in 2017 (Giechaskiel et al. 2018).

## *1.2. Definition of the problem; the need for stricter regulations*

In the existing regulations, the minimum threshold for the particle diameter is 23 nm. This lower threshold has been chosen to include the smallest possible soot particles and at the same time, exclude particles originating from volatile nucleation modes. However, concerns have been raised that this smaller size is not sufficient for many vehicle technologies as high concentrations of solid sub-23 nm particles have been measured (e.g. Giechaskiel et al. 2019). There is a strong need for a comprehensive characterisation of particle emissions for latest and upcoming vehicle technologies, especially as the European automotive sector is fighting to adapt to a global market that is irreversibly changing in favour of more environmentally friendly cars (Ortega et al. 2020). Responding to these concerns, the EU launched the GV-022016 Call for 'Technologies for low emission light duty powertrains' with a particular emphasis on measurement and characterization of sub-23 nm particles. Understanding of particle formation will support the development of future, more efficient engine and aftertreatment technologies.

## *1.3. Approach to the solution*

To investigate the technical feasibility of regulating particulate emissions sizes down to 10 nm, and to understand the physical nature of sub-23 nm emissions, the EU organised the Horizon 2020 GV-02-2016 Call. Three projects were funded in this call: DownToTen, PEMs4Nano and SUREAL-23.

In DownToTen and PEMs4Nano, sub-23 nm PN-PEMS demonstrators were developed with high efficiency in determining PN emissions of current and future engine technologies in the real world. Together with the new technology, the projects have developed robust sampling and measurement methodologies for laboratory and RDE measurements. The demonstrators were validated by applying them to current and future engine/vehicle technologies, as well as state-of-the-art exhaust aftertreatment systems in the laboratory and real-world conditions. The technical developments were supported by fundamental characterisation, to increase the understanding of the nature and the physicochemical characteristics of sub-23 nm particle emissions. Models were developed to simulate particle transformation during sampling and sample conditioning processes using experimental evidence from the project. These models can be used for model-guided application (MGA) and provide input on emissions factors for particle number emissions from current and future technologies to enhance air quality modelling tools.

SUREAL-23 focused more on overcoming the relevant barriers in the exhaust particle sampling and treatment methodology by introducing radical new technologies enabling accurate measurements down to 10nm. Such technologies may complement and extend established particle measurement protocols, sustaining the extensive investments that have already been made by the

industry and the regulatory authorities. In parallel, novel technologies for concentration, size and composition measurements were introduced to overcome the relevant barriers in the exhaust emissions measurement technology. State-of-the-art aerosol measurement techniques were advanced for better compatibility with sub-23 nm exhaust particles as well as on-board use. The developed instrumentation was used to assess sub-23 nm particle emissions from many current and future vehicle technologies accounting for effects of the fuel, lubricants, after-treatment and driving conditions. Similar to DownToTen and PEMs4Nano, SUREAL-23 systematically characterised sub-23 nm particles to facilitate future particle emission regulations and to assess any potential trade-off between advances in ICE technology towards increased efficiency and emissions.

All three projects delivered novel instrumentation for both laboratory and PEMS measurements.

### *1.4. Scope of the paper*

The scope of this paper is to i) briefly outline the main technological innovations and scientific insights from the three projects and ii) in collaboration between the European Commission (the European Commission's Directorate-General for Research and Innovation (RTD) and the European Commission's Climate, Infrastructure and Environment Executive Agency) and the projects consortia, to present project-specific conclusions and recommendations for the future regulations for particle measurements and share them with relevant policy Directorates-General as a potential basis for implementing new regulations for particulate matter and air quality.

After introducing the current state-of-the-art of particle measurement technology, the developed instrumentation as well as the results of the physicochemical characterisation will be presented. The validation of new equipment is discussed, both using laboratory and on-road measurements, together with the emission behaviour of a selection of vehicles. Finally, the conclusions and policy implications are presented.

# 2. State of the art

## *2.1. Particle measurement technologies*

The most established device to measure the particle number concentration is the Condensation Particle Counter (CPC). In a CPC, particles are exposed to a supersaturated gas from a working fluid (usually butanol, isopropyl alcohol, or water) and subsequently introduced into a condensation chamber. The vapour condenses onto the particles, so they grow to micrometre-sizes and can be optically counted. The lower detection limit is usually considered to be the size at which the CPC can detect 50% of the particles, referred to as $D_{50}$. There are several CPCs commercially available with $D_{50}$ values in the order of a few nanometers (2.5 nm). However, close to the $D_{50,}$ the counting depends strongly on the particle composition. For example, it was reported (Sakurai, 2007) that in a butanol-based CPC, the $D_{50}$ counting efficiency at 10 nm of emery oil, sucrose, sodium chloride, and ammonium sulphate aerosols varied from 0 to 65%, depending on the composition. As a result, the reference particles used for CPC calibration should be chosen carefully for size ranges close to the $D_{50}$.

The surface area of aerosols can be measured using aerosol particle charging. In the typical setup, the aerosol particles pass a diffusion charger, in which the particles are charged in a stream of ions. Subsequently, the charged particles are detected using an electrometer, a current-amplifying device. Care should be taken that the measurement is not biased by the initial charges carried by the aerosol particles (inherited from their formation mechanism), by electric fields or environmental factors that affect the reading of the electrometer. Improvements focus, among others, on redesigning the diffusion charger to minimise particle losses in the sub-23nm size range.

Aerosol particle size distributions below 1µm can be determined using a scanning mobility particle sizer (SMPS). It consists of a differential mobility analyser (DMA) coupled downstream with a CPC. The performance of most DMAs is limited for particles below 10 nm in size due to diffusive broadening of the transfer function. Nonetheless, by running the sheath flow at sufficiently large Reynolds numbers, it is possible to obtain size resolution for sizes well down to 1 nm.

Finally, composition-specific techniques can be used to determine black carbon, the organic polycyclic aromatic hydrocarbons and metals. An example is using light absorption to determine black carbon or (using several wavelengths) the content of organics (Utry, 2014). Light absorption is measured by extinction measurements, photoacoustic sensors or by photothermal interferometry. Whereas no commercial devices exist for the last technique, it has the potential of being very sensitive. Alternatively, photoelectric charging, i.e. charging the particles directly by the emission of photoelectrons due to irradiation with UV light (Burtscher, 1992) strongly depends on the particle surface. It thus can be used to monitor adsorbates (Burtscher, 1992).

## *2.2. Certified measurement devices*

Current measurement devices are certified to detect particles down to 23 nm, and the existing systems and procedures are unsuitable for detecting 10 nm particles. The reasons are two-fold. Firstly, particle losses in the size range 10-23 nm are significantly higher than for >23 nm particles, and those losses are size-dependent. Secondly, below 23 nm, a large contribution of small semi-volatile particles can be detected. Semi-volatile compounds are partially unburnt hydrocarbons resulting from fuel and oil combustion, as well as sulfuric acid particles that originate from sulphur compounds in the fuel and oil. These volatiles can strongly influence the counting of the solid particles; in the absence of an effective solution for their elimination, the particle count at 10 nm may vary by an order of magnitude.

While several strategies for removing the volatile fraction have been used in the past, the current main two include the catalytic stripper (CS), and the volatile particle remover (VPR). The CS oxidises the organic material and can store sulphur compounds. The main component of the VPR is the evaporation tube (ET), which (instead of removing material) it avoids

renucleation/condensation by evaporation. Most of these devices have high losses for the smaller particles. For example, losses in the PMP conditioning system (comprising the VPR), increase rapidly for the sub-23 nm particles (Giechaskiel, 2014a). The partial evaporation of the larger semi-volatile particles is a significant issue, especially for the VPR as these may not be completely evaporated, resulting in smaller volatile particles probably below 23 nm.

Furthermore, the VPR approach has concentration limits. Renucleation occurs after passage through the VPR when the concentration of hydrocarbons is high enough, a phenomenon that is enhanced in the presence of sulfuric acid aerosols. Also, non-volatile ultrafine particles can be produced by charring of initially volatile material in the VPR (artefact particles). In general, the CS is superior to the ET in volatile particles removal but is associated with higher particle losses.

# 3. Instrumentation for particle emission measurements focusing on sub-23 nm particles.

The three projects have advanced the available instrumentation for particle emission measurements focusing on the sub-23 nm particles. The developed technology is described per project.

### *3.1. DownToTen*

The main innovation in DownToTen is a novel sampling and measurement system for both solid and total particle numbers, with the dilution system identified as the critical component in the measurement chain. A laboratory, as well as, a portable version of a sampling system was developed, starting from fundamental investigations.

The principal chosen system was a two-stage dilution system combining a heated porous tube type primary dilution stage and an ejector type secondary dilution stage. Figure 1a shows the particle losses of the system (called HPCE, which stands for Hot Porous Cold Ejector) as function of particle size without and with two different catalytic strippers (CS1 and CS2) used in the prototype sampling system and for a version of a commercial dilution system (AVL PN PEMS with CS1). CS1 was larger than CS2 in size and also the sulfur trap capacity of CS1 was larger. Run with the same volumetric flow rate, the space velocity was lower for CS1. The inclusion of CS increases the particle losses of the smallest particles only by diffusion, and it does not affect the thermophoretic particle losses of the whole system. CS1 with a lower space velocity caused somewhat higher diffusion losses than CS2. Nevertheless, the measurements showed that the losses of the prototype HPCE system with CS1 were comparable to the commercial sampling system, designed for the measurement of non-volatile particles larger than 23 nm.

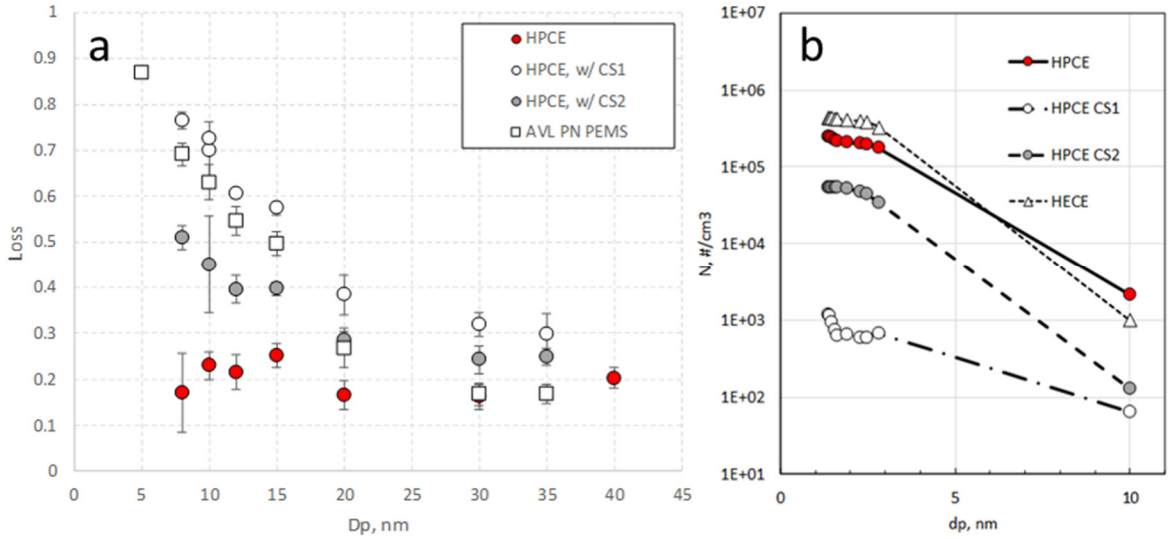


*Figure 1. (a) Particle losses as function of DMA selected particle size for HPCE (Hot Porous Cold Ejector) diluter without and with two catalytic strippers (CS1 and CS2), and for commercial dilution system (AVL PN PEMS with CS1). (b) Cumulative size distributions measured with the different sampling systems for silver particles and a GSA mole fraction of $5.7 \cdot 10^{-6}$. The graph combines data from a Particle Size Magnifier (PSM) and a 10 nm CPC (HECE: hot ejector, cold ejector – also shown for comparison).*

Also, the potential for sulfur driven nucleation mode formation and particle growth artefacts was studied, using gaseous sulfuric acid (GSA). If the GSA concentration is high enough and the condensation sink formed by pre-existing particles is low enough (sub-10 nm silver particles in this

case), sulfur-driven nucleation may take place. Another measurement artefact could be caused by the sub-10 nm silver particles growing into sizes measurable by the system. Figure 1b shows the results of such an artefact test. The cumulative count of particles larger than 1-3 nm particles did not exceed the inlet silver particle concentration, indicating that there is no tendency to form a nucleation mode. The concentration of sub-10 nm particles is the lowest for CS1 with the highest solid particle losses below 10 nm. The concentration measured at 10 nm indicate an artefact caused by silver particles grown by sulfuric acid. The artefact concentration was quite low for both systems with a catalytic stripper but especially so for the CS1 with the lowest space velocity (and the highest sulfur trap capacity). The CS incorporates a sulfur trap to minimise the risk of potential artefacts caused by $SO_2$ oxidation to sulfate particles. The sulfur trap capacity of the CS is important for long-term efficiency and resistance to artefacts, and so regeneration as part of a service schedule is recommended.

Figure.2(a and b) shows the final DownToTen portable sampling system, that includes new porous tube diluters and static mixing elements which were designed, simulated and manufactured for this purpose. The DTT system used, and built upon, the principles of the existing PMP layout, for practical and pragamatic reasons, including the minimization of complexity when amending the current regulatory text for testing and calibration.

The porous tube diluters allow for a substantial size reduction of the overall system facilitating the application of the chosen concept in a portable exhaust particle system (PEPS) configuration. The mobile system includes two CPCs, one with a d50 of 23 nm and one with a d50 of 10 nm to allow the concurrent measurement of the currently regulated particle number concentration (d > 23 nm) and the fraction between 10 nm and 23 nm.

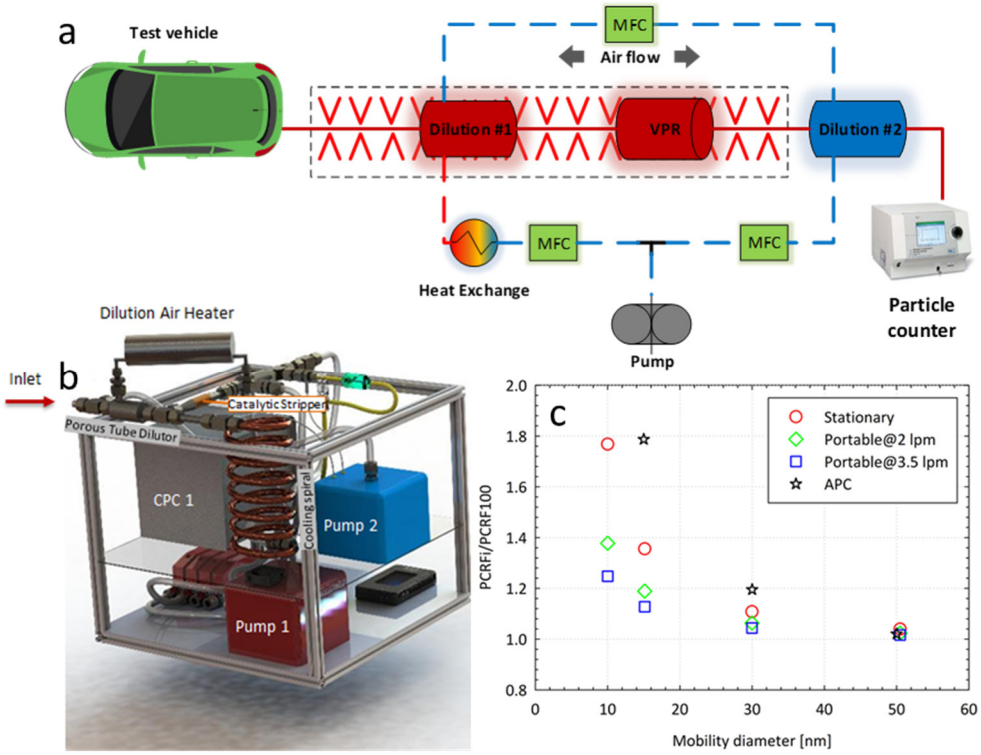


*Figure.2. (a): Scematic of the components of the DownToTen system. (b): DownToTen Portable Exhaust Particle Sampling System. The dimensions are 50 by 50 by 50 cm.(c): Losses of DownToTen systems compared with losses of commercially available AVL APC.*

Optimisation of the CS allowed for further improvement in particle penetration and thus, detection of smaller particles (Figure.2c, in most of the calibrations, two series of measurements were performed sequentially for each configuration, and the average is used). Both lab-based (stationary) and PEPS showed improvements over APC below 50 nm, whereas the PEPS showed lower losses than the stationary system. An optimised CS at higher flow provided the best performance for the portable system. The volatile particle removal efficiency remained higher than 99.99% for polydisperse emery oil particles at concentrations of 5 mg/m$^3$, which were substantially higher than required by current automotive regulations.

In addition to the PEPS, DownToTen developed a Portable Emissions accuracy Test bench (PET), an aerosol gas exchange system (AGES) for nanoparticle sampling at elevated temperatures (Bainschab, 2019), and a new mobile aerosol characterisation system (HELIOS/SCRIT) which enables highly sensitive chemical analysis of particle-associated volatile substances (Klemens et al. 2021). Moreover, a commercial AVL PN PEMS system using an Electrical Particle Counter (EPC) and a dilution concept similar to the DTT sampling system was successfully modified for 10 nm measurements. This demonstration EPC PEMS exhibited similar particle losses with the DTT PEPS, and a detection efficiency similar to that of commercial 10 nm CPCs. Finally, the DownToTen system is suitable for secondary aerosol emission characterisation measurements either by bypassing the CS or by using a separate line after the first dilution stage. Measurements with a synthetic exhaust stream showed no significant differences in the composition of the secondary aerosols for the different sampling systems (see Simonen et al., 2019, for more details on the characterisation of the secondary aerosol).

### *3.2. PEMs4Nano*

A HORIBA OBS-ONE PN 23 nm PEMS device was used as the starting point for the innovations in PEMs4Nano. Firstly, a TSI PEMS-CPC was optimised and calibrated for sub-23 nm measurements. The target of having a particle detection efficiency for thermally conditioned CAST flame soot of greater than 50% at 10 nm was achieved by adjusting the temperatures of the saturator and condenser of the instrument (saturator from 30°C to 40°C, condenser from 21°C to 20°C). A larger temperature difference between the saturator and the condenser can increase the sensitivity to smaller particles, and shifts of cut-off size from 23 nm to 10 nm.

Secondly, the integrated PEMS device was optimised and calibrated. In the system analysis, the catalytic stripper was identified as the element with the highest particle losses in the sub-23 nm regime. Being part of the volatile particle remover (VPR), the catalytic stripper is located between the first dilution and the second dilution stage. Since the goal in PEMs4Nano was to develop a system that reliably counts only the solid particles, the catalytic stripper was redesigned to remove volatiles and semi-volatiles whilst keeping the detection efficiency for sub-23 nm solid particles as high as possible, full details by Woo et al. (2021)

To achieve this, a trade-off must be made between semi-volatile removal and solid particle penetration; the two parameters have opposing trends and cannot be optimised simultaneously. Semi-volatiles typically have higher mobility than solid particles, but for sizes of 10 nm and below the mobility starts to become similar. In the trade-off, the most important criterium was to avoid homogeneous nucleation of (semi-)volatiles, whilst allowing the condensation of semi-volatiles onto solid particles. To this end, the length of the alumina monolith that houses the catalyst in the catalytic stripper was shortened by half, thereby also reducing the total number of catalyst particles by half. As Figure 3a shows, the size-dependent particle penetration was increased from 50% to 65% penetration at 10 nm. The system efficiency curve of the PEMS shows that a detection efficiency of 20% at 10 nm could be achieved (see Figure 3b). Additional potential for improvements for >20% detection efficiency at 10 nm is possible by further reducing the cut-off of the CPC and optimising the flow-dependent particle losses.

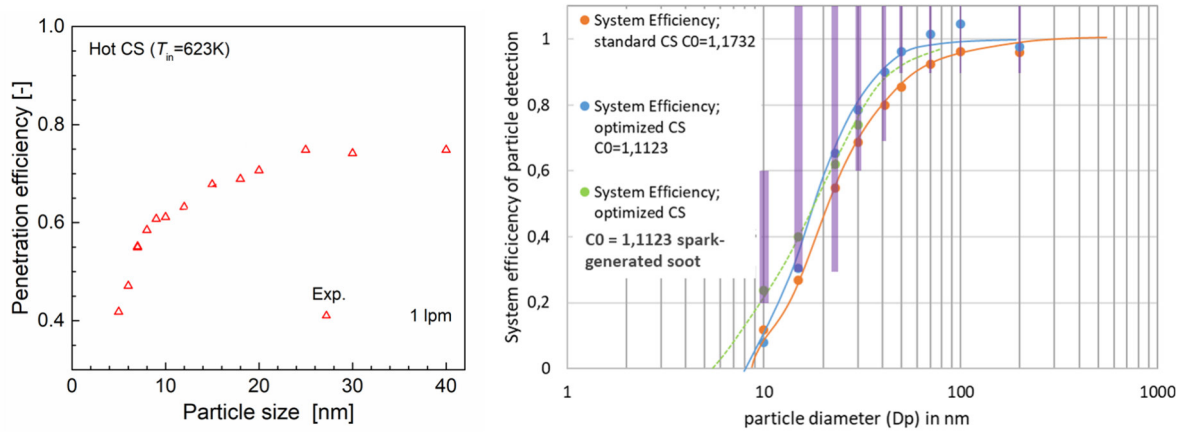


*Figure 3. (a) Measured solid particle penetration efficiency for hot operating conditions (Tin = 623K). (b) A system efficiency of > 20 % at 10nm (with spark generated soot). The purple bars indicate the set target; the performance is above target for all diameters.*

### *3.3. SUREAL-23*

SUREAL-23 attempted to overcome the unavoidable losses and artefacts the exhaust particle dilution and treatment systems bring by minimising the measurement instruments' requirements for such systems. Current measurement devices are only capable of doing measurements at room temperatures. Consequently, there is a need for dilution and taking care of the problems associated with the volatile condensation. SUREAL-23 developed two instruments, one for particle number concentration, the Induced Current Aerosol Detetector, ICAD (Fierz et al., 2014) and one for particle sizing, the Half-Mini Differential Mobility Analyser, HM-DMA, (Fernández de la Mora, 2017 and Fernández de la Mora et al., 2017) that enables hot sample (180 °C) measurements. These two instruments require no or minimal dilution (e.g. a single hot stage diluter) depending on the vehicle emission levels. For current technologies where filters are installed, both instruments can perform measurements from the raw exhaust via a simple heated line. Advantages are apparent concerning the possible losses due to the CS or the ET and the multi-stage dilution systems. Moreover, the minimal dilution system requirements enhance the on-board use of these instruments.

In Figure 4, measurements of ICAD and HM-DMA (Baltzopoulou et al., 2019) via a hot single-stage diluter are compared to measurements via a typical PMP compliant dilutions system hosting a CS. The instruments provide equivalent results in both cases.

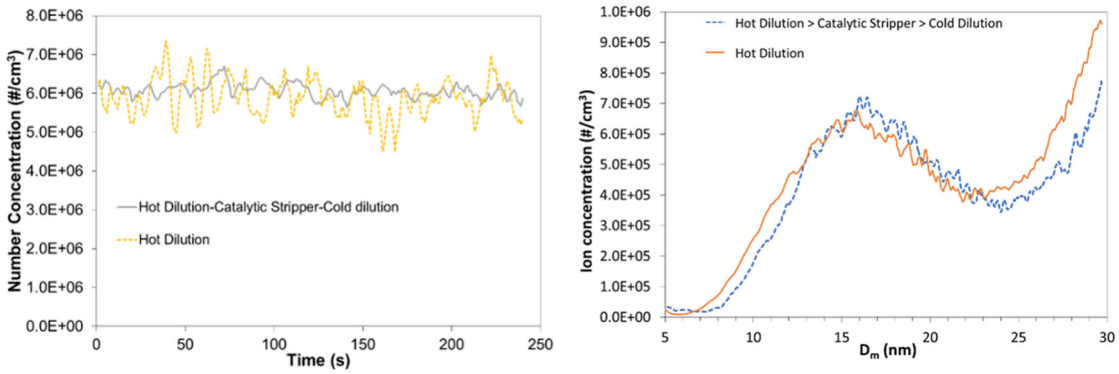


*Figure 4. Engine exhaust automotive ICAD (left) and HM-DMA (right) measurements either with a single hot dilution stage performed or downstream a PMP-compliant system (Hot Dilution>Catalytic Stripper>Cold*

*Dilution).. Tests at diesel generator operated at low load with fuel additives. The generated solid particle distribution had $D_{mean}$=40.5 nm, and 20% of the distribution lied in the sub-23 nm size range. "Hot dilution >CS >cold dilution" is PMP conform system.*

For the cases where hot sampling is not possible (e.g. instruments other than the ICAD and HM-DMA) SUREAL-23 developed an advanced sampling and conditioning particle system, specially designed for sub-23 nm solid particles (Chasapidis et al., 2019). The dilution process is achieved in two stages; the primary dilution is done with a porous tube while the secondary with an ejector diluter that also acts as a pump for the sampling flow. The system offers flexibility in terms of dilution ratio (DR), which is calculated in real-time with an algorithm based on a differential pressure measurement across an orifice. Between the two dilution stages, a catalytic stripper removes the volatile material. The system combines high stability of the DR with >99% volatile particle removal and a cut-off size ($d_{50}$) at 7.5 nm. The central part of the dilution system is the CS which manages to offer high catalytic function efficiency (>99% removal of tetracontane particles) with sulphur trapping capability (complete Sulphur removal during many hours of operation) as well as low particle losses. Specifically, for the stand-alone CS, penetration even down to 10 nm remains relatively high and equal to 0.81. The average particle number concentration factor, PCRF, was calculated accordingly to include particles down to 10 nm and was found to be 1.18 ((Melas et al., 2020).

In addition, a variable wavelength ultra-violet photoelectric charger (UV-PEC) was developed for on-line/in-situ composition analysis of sub-23 nm particulate emissions.

# 4. Nature of sub-23 nm particles

Together with developing instrumentation, the nature of sub-23 nm particles has been studied.

### *4.1. DownToTen*

DownToTen focused on three cases that are known to produce higher amounts of particles and: cold start operation, DPF regeneration events and high speed accelerations and attempted to characterize them and investigate their origin.

Cold start emissions, from the first two minutes following crank, are shown in Figure 5. Except for one test on a GDI with TWC and GPF, the only vehicles emitting below the Euro 6 limit, for >23nm particles, are DPF-equipped diesels. Since there is an on going discussion for the contribution of short-duration cold start phases to the overall cycle results, data are shown normalized to the Euro 6 limit value, to put the emissions magnitude into context. It should be noted that control of PN emissions from cold start events in isolation is not advocated.

In comparison with Figure 14, Figure 5 shows a much larger number of results lying outside the green zone (which includes PN23 and PN10 emission results below the current PN23 limit), and much higher emissions levels – in some cases approaching 100x the regulatory limit value. This indicates that despite some very high cold start levels, particle emissions during drive cycles reduce substantially after cold start, and enable most vehicles and drive cycles to meet the limit. Clearly, in applications with high cold start emissions, shorter cycles will be more challenging. Considering the cold start emissions results that are greater than the Euro 6c limit, the highest emissions are seen from a wide-open throttle acceleration on a TWC-equipped GDI. This test produced emissions of ~85 times the Euro 6 limit for PN10 and about half that for PN23. These emissions were almost certainly dominated by soot particles generated under fuel-rich conditions.

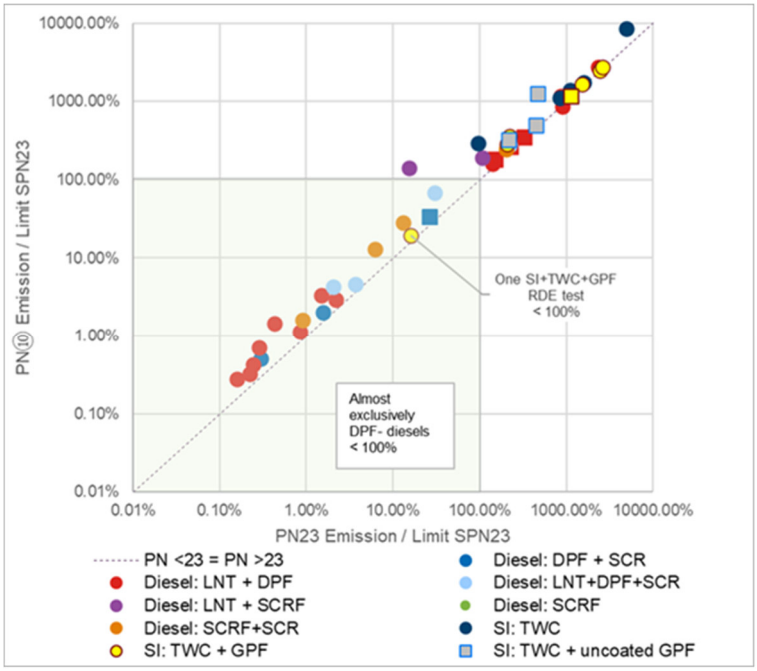


*Figure 5 Cold Start PN emissions from PN23 and PN10 measurements – standard drive cycles*

Diesel PN emissions from active regenerations can be dominated by PN<10 for short periods. In the example of Figure 6, about 100s after the post-injection event commences (at about 930s), there is a sharp rise in PN>23, indicating that soot combustion has commenced and DPF filtration efficiency is reduced. At this time, >7nm emissions are relatively similar to >23nm levels. About a minute later, as the regeneration event continues, emissions of >7nm particles increase more rapidly than those >23nm and the real-time profiles diverge. This continues for ~260s, during which >7nm PN emissions reach ~30 times the levels of >23nm particles. These particles may derive from partially combusted <23nm soot, but are more likely created by the release of ash from the DPF via thermo-diffusion from the within substrate walls or possibly through gaseous release via localized volatilization and recondensation, as at around 400s after the post-injection started, the >7nm and >23nm converge, but >23nm PN have not reached a minimum. It seems likely that the >7nm PN are released rather than created from soot, as consistent conditions within the DPF during the regeneration would be expected to continue producing <23nm soot throughout the post-injection, if this was a significant mechanism. These PN<10 emissions may derive from oil additive metals converted to metal oxides in prior operation and released during the regeneration event.

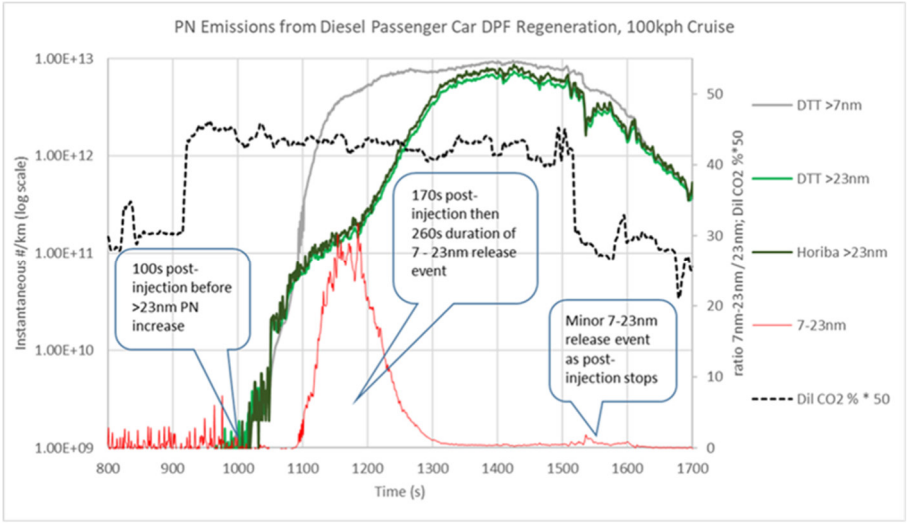


*Figure 6. PN Emissions during an active regeneration on a Euro 6d DPF-equipped Diesel Vehicle. The test vehicle was accelerated to 100kph and after ~900s the regeneration triggered. The test was terminated after ~2350s, when PN had stabilized. PN was measured by a production (Horiba) and the DownToTen prototype >23nm and >7nm systems*

GDI engines may emit <23 nm soot particles under very high load transients (Figure 7). These particles exist in a minor mode with a peak at ~20 nm within which almost all particles are above 10 nm. Due to high concentrations in the second (soot/accumulation) mode, it is unlikely that the minor mode is solely ash materials, and most likely it is comprised of primary carbon particles. This is consistent with poor fuel-air mixing and possible fuel impingement, leading to pool fires and carbon formation. The highly dynamic operation of the engine may restrict soot formation to local regions but also mobilise this soot very rapidly, leading to limited agglomeration and a higher number of primary carbon particles.

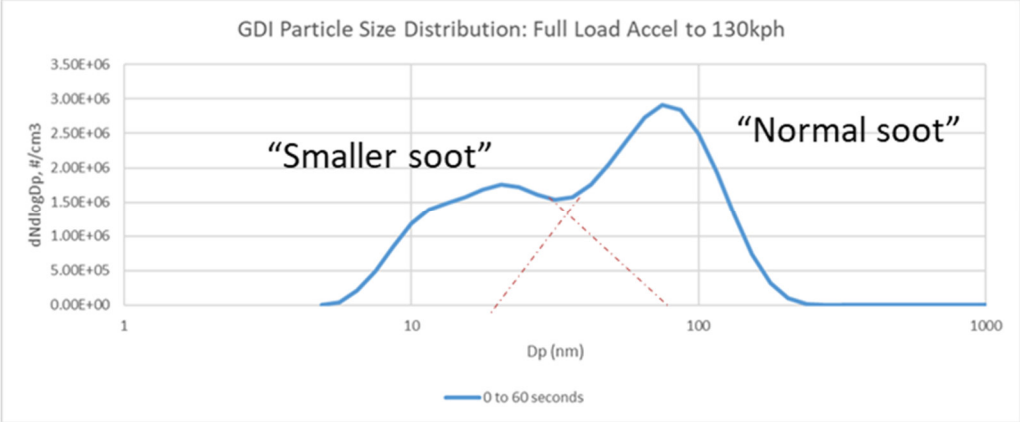


*Figure 7. Particle size distribution measured (with a Cambustion DMS500) during full load acceleration on a GDI vehicle.*

### *4.2. PEMs4Nano*

A thorough physicochemical characterisation of size-selected nanoparticles emitted by a gasoline direct injection engine was performed in PEMs4Nano (Focsa et al., 2020). Particles were sampled from the engine exhaust (with the engine operated in various working regimes) and separated into different size-bins for subsequent analysis (without altering their chemical composition due to their condensation during collection). The morphology and nanostructure were studied on individual particles by transmission electron microscopy (TEM) and atomic force microscopy/tip enhanced Raman spectrometry (AFM/TERS). These measurements demonstrate the ability, not only to detect solid particles as small as 6 nm (Figure.8), but also to unambiguously identify them as soot particles because of their unique Raman signatures (D and G bands) and turbostratic nanostructure. To the best of our knowledge, these measurements are the first TERS measurements on ultra-fine combustion-generated particulate matter.

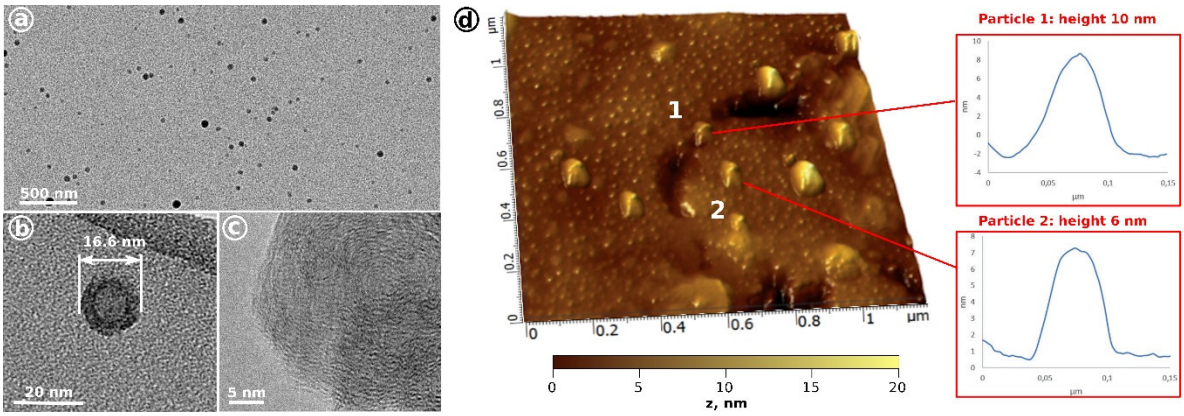


*Figure.8. Structure and morphology of ultrafine particles as revealed by TEM images and AFM topographic mapping. (a), (b), and (c) various magnification TEM images of size-selected soot particles (18 nm (±5nm)) collected in a high load engine regime with a DMA-NAS arrangement (nano-DMA, TSI Inc., Model 3085, and nanometer aerosol sampler, NAS; TSI Inc., Model 3089) on SiN membrane (Norcada, Model NT050Z). (a) and (b) show that the collected (primary soot) particles exhibit spherical shapes. (c) High-resolution TEM image revealing the turbostratic internal structure characteristic of soot particles. (d) Topography image (1.2 x 1.2 μm$^2$) of nanoparticles collected on gold-coated Si wafers (EMS, 71892-10) obtained with AFM and particles 1 and 2 corresponding topographic cross-sections.*

TERS measurements (Focsa et al., 2020) show great diversity (at least in terms of nanostructure) within soot particles yet belonging to the same same size bin and generated by the same engine with identical operating conditions. This finding is crucial for interpreting the off-line chemical composition measurements that were carried out by two-step laser mass spectrometry (Popovicheva et al., 2017; Faccinetto et al., 2015) and secondary ion mass spectrometry (Irimiea et al., 2019). The properties and trends derived from the chemical composition analyses are statistically significant as they are averaged over many (differently sized) particles, and therefore offer valuable input for the theoretical model, which utilizes statistical approaches on particles ensembles (Lee et al., 2019).

The combination of mass spectrometry and advanced statistical procedures clearly shows that the chemical composition varies with the particle size (Focsa et al., 2020; Duca et al., 2019). Characterising particulate matter on such a molecular level made it possible to identify key chemical markers, based on which in turn the main production source could be identified (fuel, lubricant, engine wear) as well as malfunctions and the engine operating regime. A clear relationship was observed between the elemental carbon (EC) content and carbon clusters, as well as an excellent correlation between the organic carbon (OC) content, the volatility, and the presence of aromatic species. The aromatic species proved to be the main chemical markers for the volatile organic fraction. The OC-EC partition was additionally shown to vary with particle size or engine regime.

The CS efficiency was assessed by measuring the volatile organic fraction. An original two-filter system (Ngo et al., 2020) was developed to sample simultaneously the gas phase and the particulate matter from the exhaust, yet on separate substrates. Mass spectrometry analyses showed that the catalytic stripper effectively removed the organic content regardless of the phase (gas or particles), as demonstrated by a drastic reduction (more than one order of magnitude) of the recorded total ion count. It was discovered that the smallest particles (10-32 nm) are the most affected by the catalytic stripper (Figure.9), indicating that particles in this size range hold a larger volatile fraction.

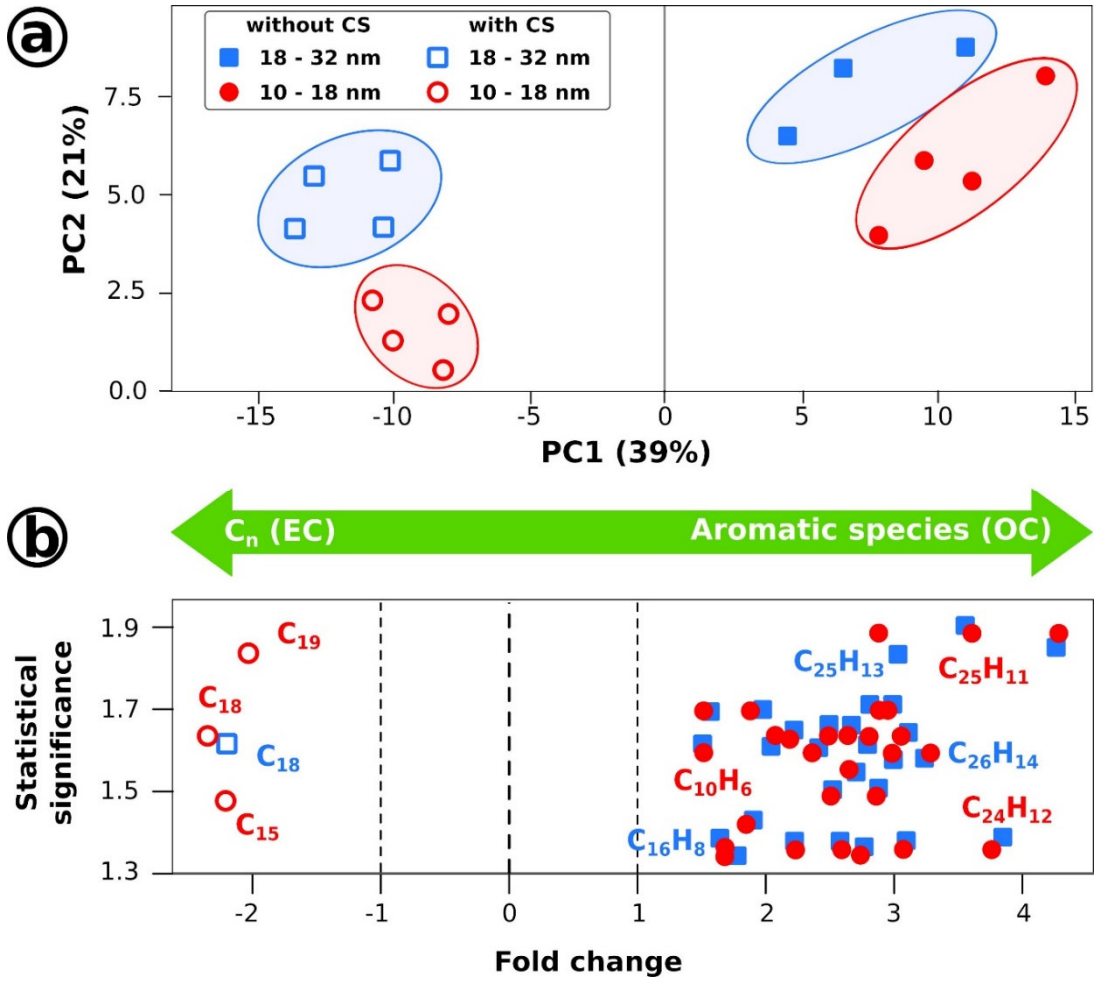


*Figure.9. Volatile organic fraction removal by the catalytic stripper as revealed by mass spectrometry and advanced statistical analysis. (a) Principal component analysis performed on mass spectra of stripped and non-stripped particles collected in the same engine regime (normal operation, high load). The first principal component (PC1) is associated with the strongest variations within the dataset and, in this case, reveals that the main change to the chemical composition induced by the catalytic stripper is a significant reduction in the contribution from aromatic compounds. The nature of the chemical species that were successfully removed from nanoparticles by the catalytic stripper is visualised with a volcano plot (b) – a scatter plot used to identify meaningful changes in large datasets. It reveals that the stripper is efficiently removing the organic content, leaving behind only elemental carbon (for which carbon clusters are marker species). Note that only compounds related to statistically significant changes in the dataset are shown (p-value lower than 0.05).*

The same behaviour was observed in on-line tandem measurements of the aerodynamic diameter-mass-mobility diameter. Figure 10(a) shows the volatile mass fraction of particles as a function of particle mobility diameter. It is evident that smaller particles have a higher volatile mass fraction. Semi-volatile compounds are ~20% of total particle mass (non-volatile core and volatile coating) for 30-nm diameter particles and only ~3% for 110-nm particles. For more details, see Kazemimanesh et al., 2021 and Duca et al., 2021. The observed trend is consistent with previous reports on PM emissions from different engines (Graves et al. 2015; Momenimovahed and Olfert, 2015; Sakurai et al., 2003; Ristimäki et al., 2007).

Finally, the behaviour is captured via the MGA workflow consisting of *k*inetics & SRM Engine Suite [Etheridge et al. 2011] for physicochemical modelling and MoDS [Yu et al. 2020] for parameter estimation and surrogate model generation. The workflow is validated against measurements for particle size distributions at multiple load-speed engine operating conditions. As the sampling conditions can influence measurements of particle size distributions mainly attributed to the amount of absorbed SOF (soluble organic fraction) and liquid condensates, a reactor network model was used to simulate the sampling system. The reactor network takes into account the cooling effect caused by the two-stage dilution air and simulates the condensation of SOF on the particles. [Lee et al. 2019]

Figure 11 shows the surface-organic mass fraction for a range of dilution ratios. The plot shows that SOF mass fraction increases with decreasing particle size, which is consistent with the aerodynamic mass-mobility measurements. The MGA also provides the sensitivity of particle size distributions and SOF mass fractions to experimental design parameters such as the dilution ratio of the sampling configuration.

The excellent agreement between independent chemical, physical, and theoretical characterisations confirms that the volatile mass fraction consistently decreases with the particle size. These findings also highlight that for particles with a non-volatile core, the semi-volatile material may represent a significant fraction of the overall particle mass. Finally, the results show the importance of stripping the semi-volatiles and that the CS is key to a robust measurement of sub-23 nm particulate matter.

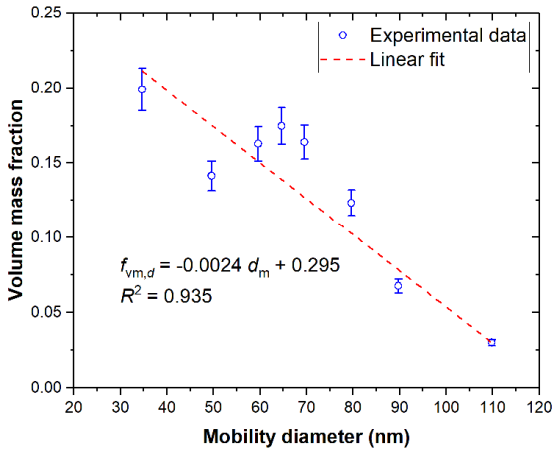


*Figure 10. Particle mobility measurements show that the volatile mass fraction (fvm,d) of particles decreases as a function of the mobility diameter (engine speed 1200 RPM, load 12 bar).*

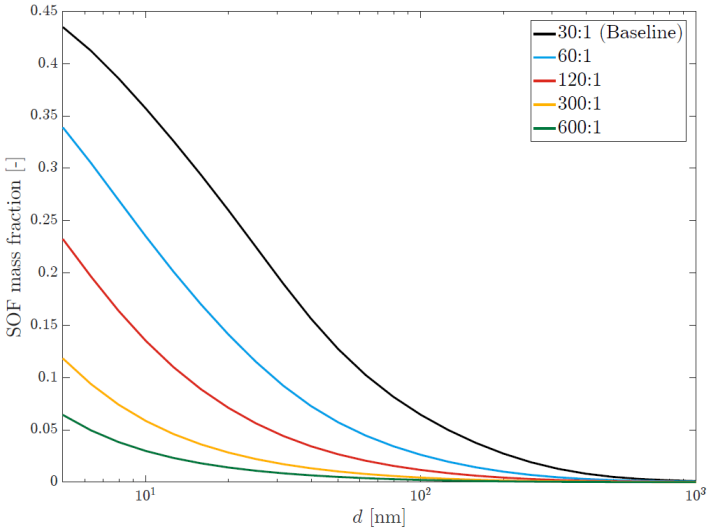


*Figure 11: SOF mass fractions for a range of dilution ratios, provided by the MGA at different dilutions ratios (colours 30:1 to 600:1) The SOF mass fraction increases with decreasing particle size, which is consistent with the aerodynamic mass-mobility measurements.*

### *4.3. SUREAL-23*

SUREAL-23 followed a comprehensive approach to study the effect of engine technology, operating conditions and fuels/lubricants on the fraction of sub-23 nm particles as well as the volatile and non-volatile content of the emitted aerosols. A variety of commercial and prototype engines and particle generators were used for the study.

#### *4.3.1. Diesel*

For Diesel, it was verified that sub-23 nm particles are not an issue, except for extreme conditions such as extreme lube-oil fuel consumption and grossly excessive dosages of fuel additives. In the case of DPF regeneration, some solid sub-23 particles have been measured, immediately after the regeneration phase, but are not considered to be a significant problem since the regeneration usually only takes a short time. Regarding the SCR function, a 3-liter engine showed a significant increase, more than 50 %, in total particles emitted, including sub-23 nm, during urea injection at medium speed and load. 3WCs have a minimal effect on particulate emissions, in contrast to particle filters, both DPFs and GPFs, which can be a very efficient means for particle number reductions, especially for sub-23 nm particles. Regarding the effect of biodiesel content in Diesel, it was observed that increasing rapeseed methyl ester (RME) content in the fuel led to increased sub-23 nm particle emissions, contrary to the total particle number.

#### *4.3.2. Gasoline*

Gasoline DI results in significantly higher total and sub-23 nm solid particle emissions than PFI. Additionally, increasing the engine speed leads to a general increase in particle emissions, including sub-23 nm particles, while the fraction of sub-23 to total particles may decrease. On the other hand, increasing engine load leads to a decrease, in general, of particle emissions; however, particles become more volatile. The increase of the ethanol content may also lead to a reduction in the total particle number as well as in the volatile content of the particles, but the sub-23 nm fraction may increase. This observation is very distinct in the pure ethanol case. The ethanol content was also assessed with the UV-PEC. As demonstrated in Figure 12, E25 fuel exhibited higher UV-PEC signal - mainly at a wavelength of 205 nm that corresponds to the photoemission threshold of PAH compounds - compared to pure gasoline. In the E25 case, emissions downstream TWC showed a sharp increase of UV-PEC signal, while downstream CS showed a decrease. This experimental

observation revealed the presence of semi-volatile fraction - relevant to PAHs - downstream TWC and the efficient stripping achieved downstream CS. Concerning E0 fuel no influence of the UV-PEC signal was observed regardless of the implementation of TWC & CS as expected due to lack of polyaromatic content in the fuel.

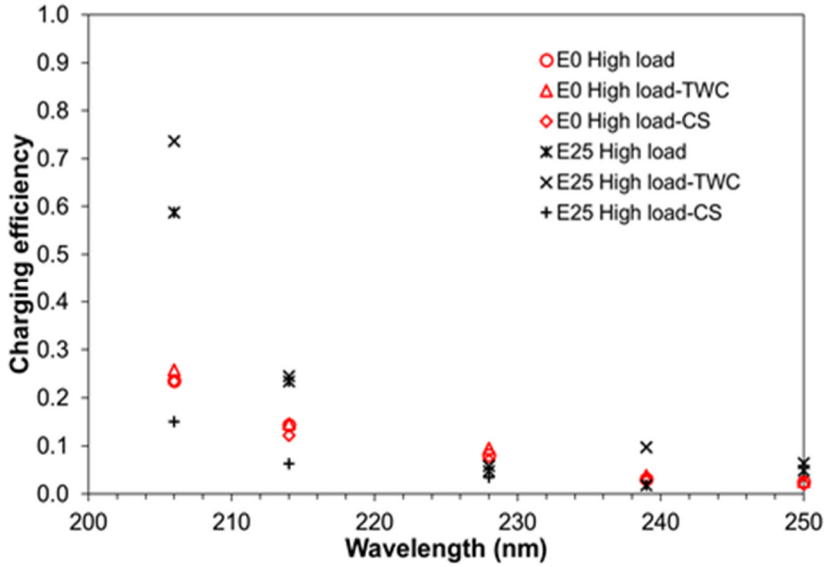


*Figure 12. Effect of ethanol content on the charging efficiency of GDI particles.*

For both PFI and DI, at high engine load, a higher volatile organic fraction (VOF) was observed compared to low load, likely due to the larger fuel supply and less time for evaporation. Engine cold start may lead to 5× or more particle emissions than those emitted under hot engine start. Total particle number and sub-23 nm fraction increase with increasing driving aggressiveness. For example, particle emissions, including sub-23 nm, are more than double for the RTS95 compared to the WLTC.

The high sulphur fuel is not causing a significant increase in particle emissions. However, the 10-23nm particle fraction is also increased compared to low-sulphur fuel. On the contrary, the high aromatic content of gasoline causes a significant increase in particle emissions. They are increased three-four times compared to all other measurement methodologies. Nevertheless, it seems that this increase comes more from the accumulation particles rather than the nucleation particles as the 10-23 nm particle fraction is the lowest among the cases studied. The effect of the lube oil content in SAPS (Sulphated Ash, Phosphorus and Sulfur) was also studied. Full-SAPS oil seems to moderately increase particle emissions, both >23 nm and >10 nm.

### *4.3.3. CNG*

In CNG engines, the exhaust particle emissions are mainly ascribed to the lube oil coming from the crankcase ventilation, the valve steam, the piston-liner system and the turbocharger system. To investigate the contribution of lube oil and fuel the particle, emissions were measured at the exhaust of an optical engine which is equipped with auto lubricating Teflon Bronze rings and it is oil free. The engine is a small displacement 4-stroke, single cylinder, port-fuel injected, SI engine fueled with CNG (CO2 1%, N2 2%, C3H8 2%, C2H6 7%, CH4 88%). The oil was added in different percentage: 1%, representative of the consumption during transient operating conditions, 3%, 5% and 7%, to provide a relation between the particle emissions and the amount of oil.

With the oil addition the number of the sub-23 nm particles increases, it reaches a maximum for the 3% of oil content, then slightly decreases remaining, however, higher with respect to the oil free condition, as presented in Figure 13. Regarding the particles larger than 23 nm, their concentration increases with the oil content even if for levels of oil greater than 3% the number augments more slowly. The tests were performed at 2000 rpm full load, chosen as representative of urban conditions.

At the increase of the oil content both the number and the diameter of particles increase resulting in a shift of the PSDF towards larger diameter. The oil contributes to the formation of pool-fire which, burning in a diffusive way, enhances the particle formation. As the oil content increases this phenomenon is stronger and the agglomeration of the particles prevails leading to the emissions of larger particles.

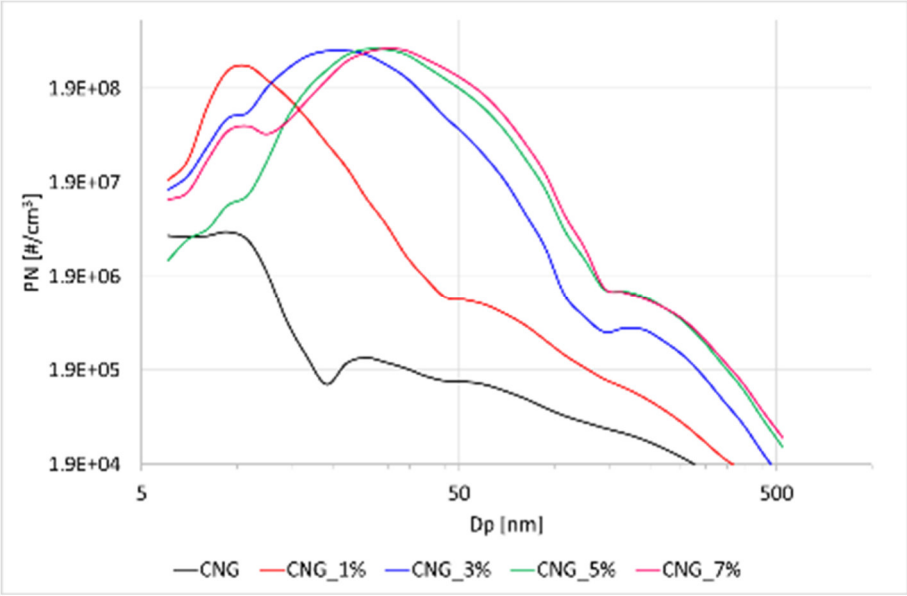


*Figure 13 Particle size distribution over the all size range using CNG fuel with diferent lubricant oil concentrations.*

# 5. Lab measurements

## *5.1. DownToTen results*

Particle production events were explored by testing a variety of engine and exhaust aftertreatment technologies and emissions certification standards (Euro 5 through to Euro VI-C and Euro 6d-Final) on a wide range of global regulatory cycles, discrete operating conditions and pre-selected speed & load patterns (beyond the boundaries of regulatory cycles). In addition, temperature, emission control regeneration and hybrid states of charge were varied.

Results are shown in a normalised format where the x-axis of the chart shows emissions of non-volatile particles >23 nm (PN23 or SPN23) divided by the current PN23 regulatory limit value ($6x10^{11}$ #/km). The y-axis shows emissions of non-volatile particles, either with a lower size threshold of 10 nm (PN10 or SPN10) or with a lower size threshold of < 10 nm (PN<10 or SPN<10), similarly normalised to the current PN23 limit value. The PN<10 data contain data measured with particle counters with 7 nm, 4 nm and 2.5 nm d50 cut-points. Engine technologies in these figures can be identified by the shape of the marker. The data shown in Figure 14 contains approximately 260

separate results for PN23 and PN10, covering 5+ orders of magnitude, and almost 220 individual results in SPN<10 data.

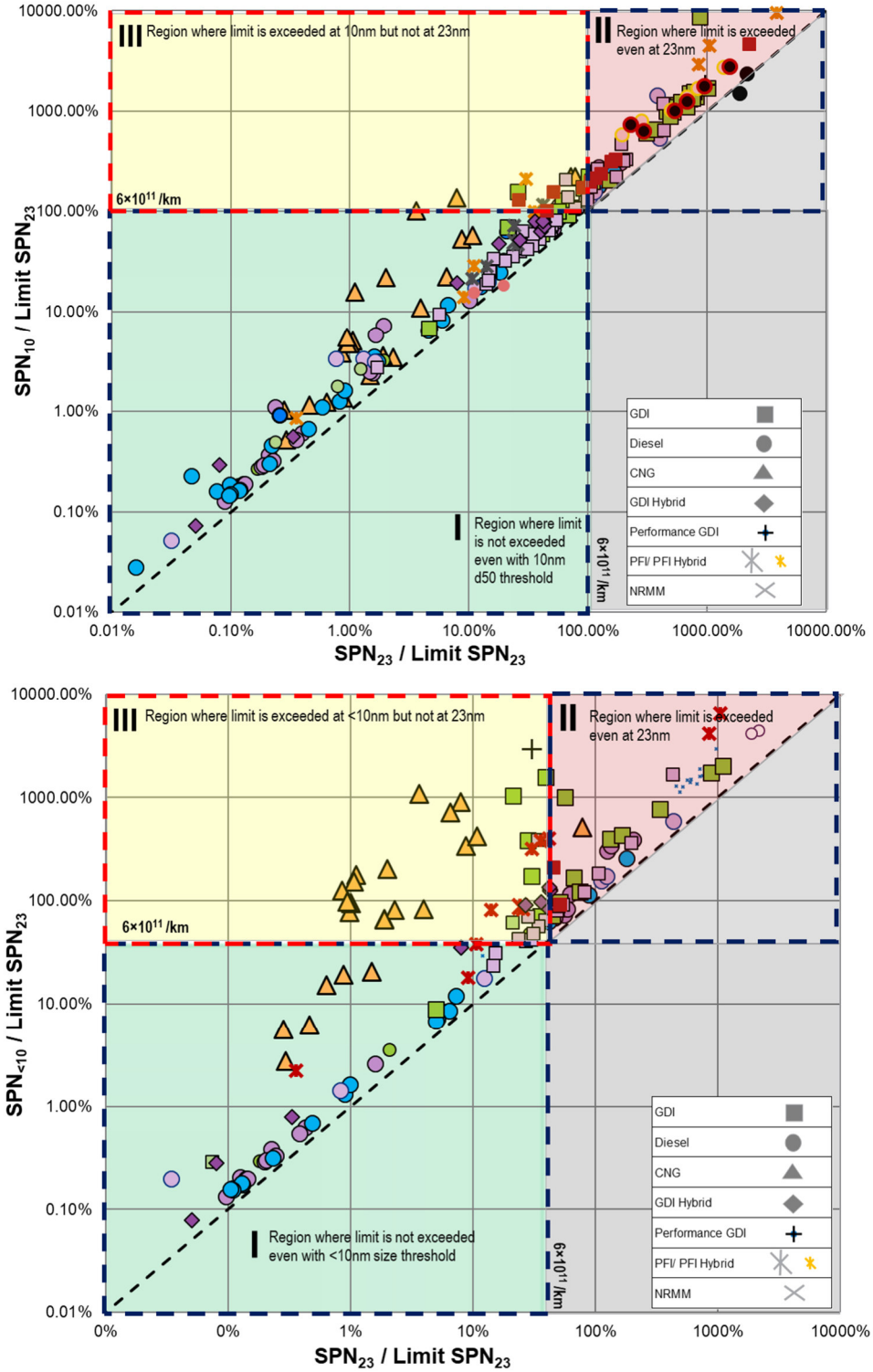


*Figure 14. All Data gathered in DTT presented in the normalised form. Note: emission data are corrected for particle losses.*

Results in Figure 14 can be identified to lie within one of three regions: Region I where emissions of both PN23 and PN10/PN<23 are below the current PN23 limit value for PN, Region II where both PN23 and PN10/PN<10 emissions are greater than the current PN23 limit value and Region III where emissions of PN23 are compliant with the current limit value, but emissions of PN10 or PN<10 exceed the PN23 limit value. As a first general observation, PN23 and PN10 results correlate well over several orders of magnitude with an offset due to the inclusion of more particles in the case of PN10 emissions. This offset varies among the different engine/powertrain and aftertreatment technologies as further analyzed in the following paragraphs. Most technologies are below the $6x10^{11}$ #/km PN23 limit for both >23 nm and >10 nm, but there are technologies with PN<23 emissions that should be targeted for further development effort to bring results into Region I. These technologies include motorcycles and mopeds, PFI and GDI vehicles without GPFs and DPF-equipped diesel after regeneration. GDI hybrid emissions are at the borderline without the GPF or fail at PN23 as well as PN10. Also GDI vehicles with GPFs are found above the limit for PN10, when the GPFs are 'fresh', i.e. where ash accumulation is minimal, and filtration efficiency is at lowest possible levels. The CNG PN emissions are significantly elevated below 10 nm, with on average 90 times as many particles when extending downwards to 2.5 nm (ratio of PN2.5/PN23nm). For more detailed discussion regarding the particle emission performance of CNG vehicles, please see Samaras et al.(2020) and Toumasatos et al. (2020).

Different technologies can be compared on a like-for-like basis using WLTC data (Figure 15). These WLTC results are consistent with the general trends of the data shown in Table 1, including the benefits of particle traps on diesel, GDI and CNG. Note that average values for some categories in the table are derived from very limited data, and the table should be considered indicative of technology effects only. Particle filters need to be improved to bring PN10 emissions below the limit in severe as well as moderate drive cycles, with a suitable engineering safety margin. This also should bring PN<10 below, or close to, the limit value. Apart from GDIs and Diesels without GPF and DPF respectively, the highest emissions are observed from the PFI applications (passenger cars and motorcycles) that are not currently subject to PN legislation, so further technology improvement, possibly involving the use of particle filters may be required. Interestingly, retrofitting of a GPF to a CNG and PFI vehicles, just for experimentation, has been seen to reduce both PN10 and PN<10 to well below the limit value (indicated as Gas+GF and PFI+GPF in Table 1). Average PN emissions from gasoline hybrids in the ICE mode under severe operating conditions will be sufficiently high to require GPFs to meet $6x10^{11}$#/km, even for PN23.

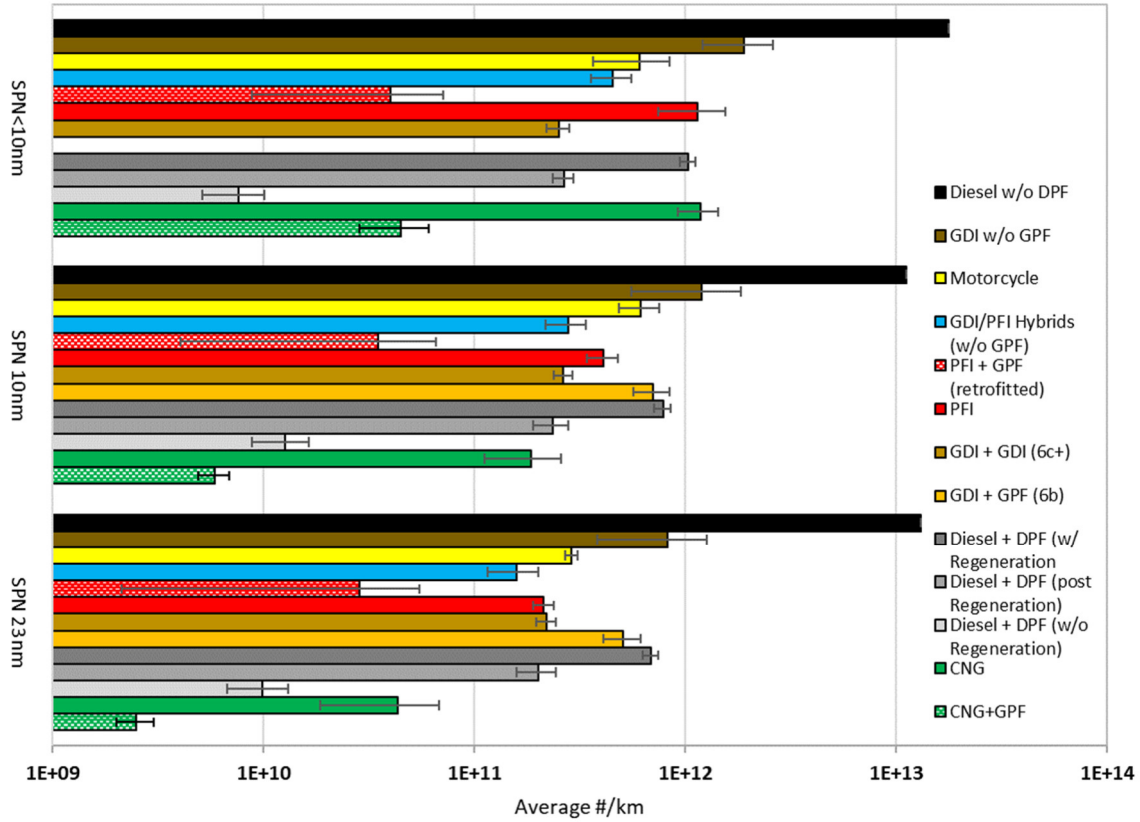


*Figure 15. A comparison of WLTC and WMTC (for motorcycle) average #/km emissions by technology. The comparison clearly shows the benefits of particle traps on diesel, GDI and CNG.*

*Table 1. WLTC and WMTC (for motorcycle) average #/km emissions by technology. Red cells highlight averages above $6x10^{11}$#/km and green cells averages that are below. It is clear that in normal operation, drive cycle emissions of applications with particle filters are always below, or close to, the limit value.*

| | SPN 23nm | SPN 10nm | SPN<10nm |
|---|---|---|---|
| CNG+GPF | 2.5E+09 | 5.9E+09 | 4.5E+10 |
| CNG | 4.3E+10 | 1.8E+11 | 1.2E+12 |
| Diesel + DPF (w/o Regeneration) | 9.9E+09 | 1.3E+10 | 7.6E+09 |
| Diesel + DPF (post Regeneration) | 4.3E+10 | 4.5E+10 | 3.1E+10 |
| Diesel + DPF (w/ Regeneration) | 6.9E+11 | 7.8E+11 | 1.0E+12 |
| GDI + GPF (6b) | 5.1E+11 | 7.0E+11 | **no data** |
| GDI + GPF (6c+) | 2.2E+11 | 2.6E+11 | 2.5E+11 |
| PFI | 2.1E+11 | 4.1E+11 | 1.1E+12 |
| PFI + GPF (retrofitted) | 2.9E+10 | 3.5E+10 | 4.0E+10 |
| GDI/PFI Hybrids (w/o GPF) | 1.6E+11 | 2.8E+11 | 4.5E+11 |

| | | | |
|---|---|---|---|
| Motorcycle | 2.9E+11 | 6.2E+11 | 6.1E+11 |
| GDI w/o GPF | 8.2E+11 | 1.2E+12 | 1.9E+12 |
| Diesel w/o DPF | 1.3E+13 | 1.1E+13 | 1.8E+13 |

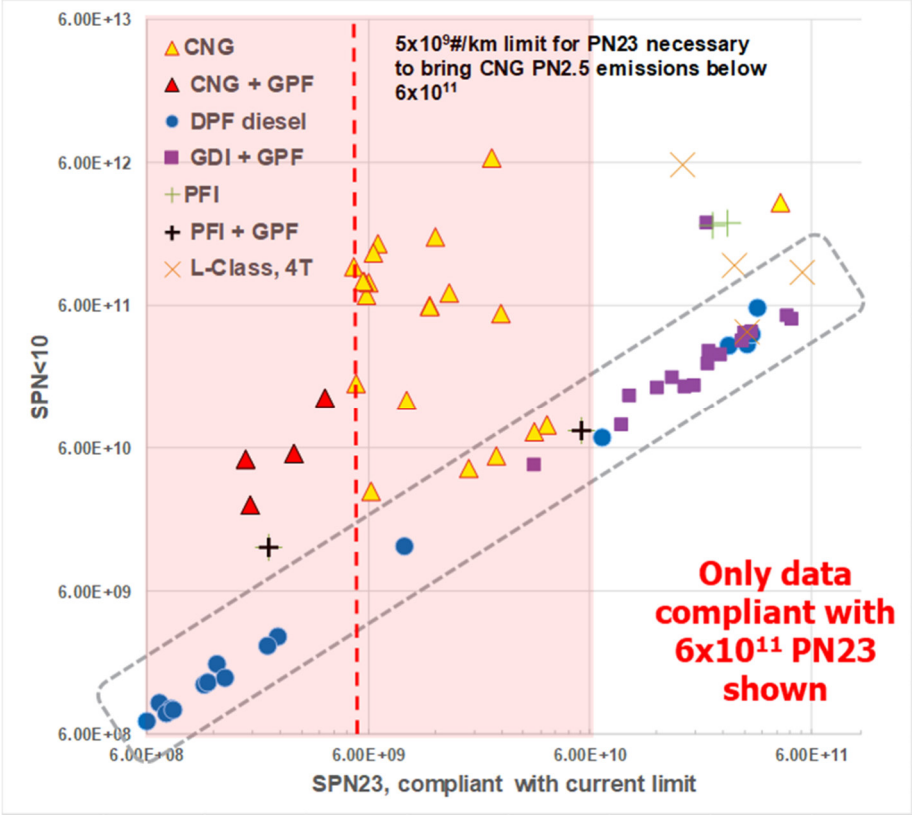

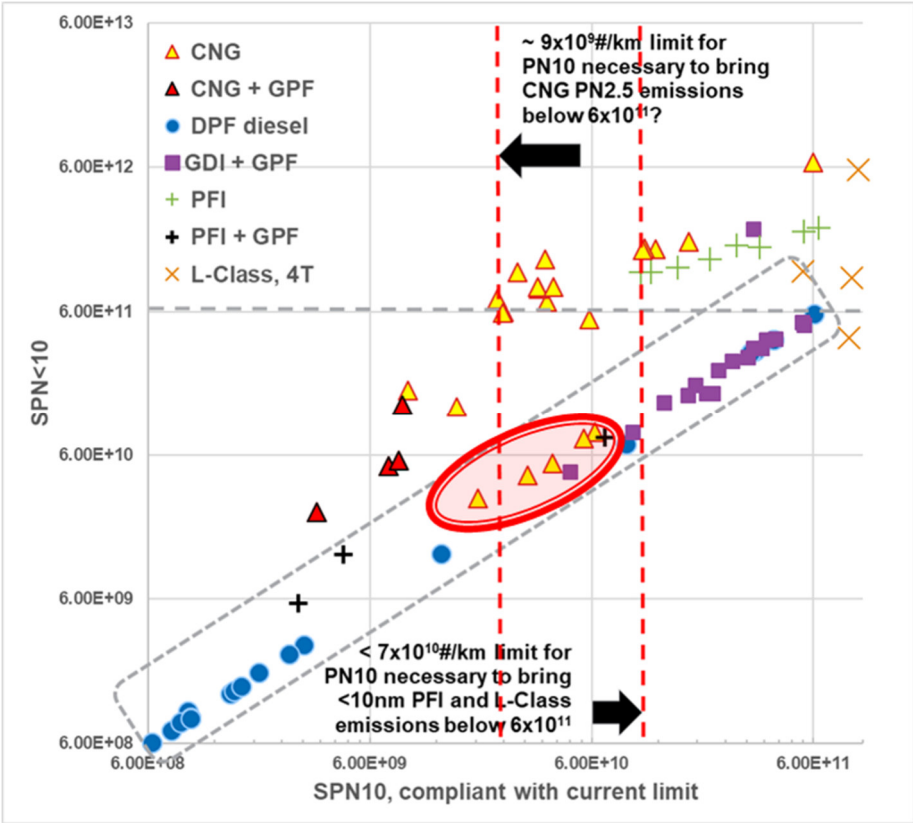


*Figure 16 (a) above: relationship between SPN23 and SPN<10 emissions (b) below: relationship between SPN10 and SPN<10 emissions. Data in the red eclipse refer to a prototype CNG vehicle without GPF from the H2020 project GasOn. For both figures data refer only to tests compliant with the 6x10$^{11}$#/km limit.*

Figure 16 reveals the possible repercussions of the size threshold on the applicable size limit. The analysis focuses only on emission data from tests compliant with the 6x10$^{11}$#/km limit. Figure 16a shows that PN<10nm and PN23nm appear to correlate for some technologies: Diesel and GDI with DPF, one prototype CNG w/o GPF (from the H2020 project GasOn), one PFI with retrofit GPF. This correlation defines desirable behaviour of technologies. Some do not comply though, in particular, other CNG with TWC, production CNG with retrofit particle filter, PFI (including with GPF), L-class 4-stroke applications. Technologies with high engine-out <10nm PN emissions appear problematic for setting a limit value (CNG could require 5x10$^{9}$ #/km at 23nm to force PN<10 below 6x10$^{11}$ #/km).

Figure 16b shows that the same type of desirable correlation exists for PN10 versus PN<10, as with PN23 and PN<10. In this context CNG, L-class 4-stroke and PFI applications show PN<10 emissions above 6x10$^{11}$ #/km. A limit of ~6x10$^{10}$ #/km would appear to require filters on PFI and L-Class 4-strokes, and could ensure GDI GPF robustness. This limit does not seem to suffice to force filters on CNG and ensure their PN<10 emissions were below 6x10$^{11}$ #/km. Moreover, a <10$^{10}$ #/km PN10 limit seems to be required to bring PN<10 from all CNG tested below 6x10$^{11}$ #/km. Interestingly, the test data from a Euro 6d-temp CNG vehicle (the H2020 GasOn technology) revealed SPN>2.5nm levels below the current regulation limit in several test cycles, even without the use of a particle filter, and hence may indicate a route to achieving low <10nm PN emissions without a filter.

The total particle number (TPN) emissions may provide an alternative to the regulated gravimetric PM mass method. TPN emissions were studied by implementing different temperature conditions and by removing the CS, as well as by evaluating different engine technologies, fuels and aftertreatment devices. Figure 17 summarises the results. Recent technologies seem to lead to

significant reductions in TPN emissions. Region I in *Figure 17* designates the region where TPN emissions are less than an order of magnitude higher than SPN emissions, including CNG, PFI, PHEV in the EV mode, alkylate gasoline (which would be expected to produce lower levels of soot in combustion, and >23nm PN) and gasoline+MMT (known to generate <20nm solid nanoparticles). However, special driving events can significantly increase these emissions as can be seen in Region II, which designates the region where TPN emissions are more than an order of magnitude higher than SPN emissions (CNG with and without PF, PFI with PF and PHEV in the HEV mode).

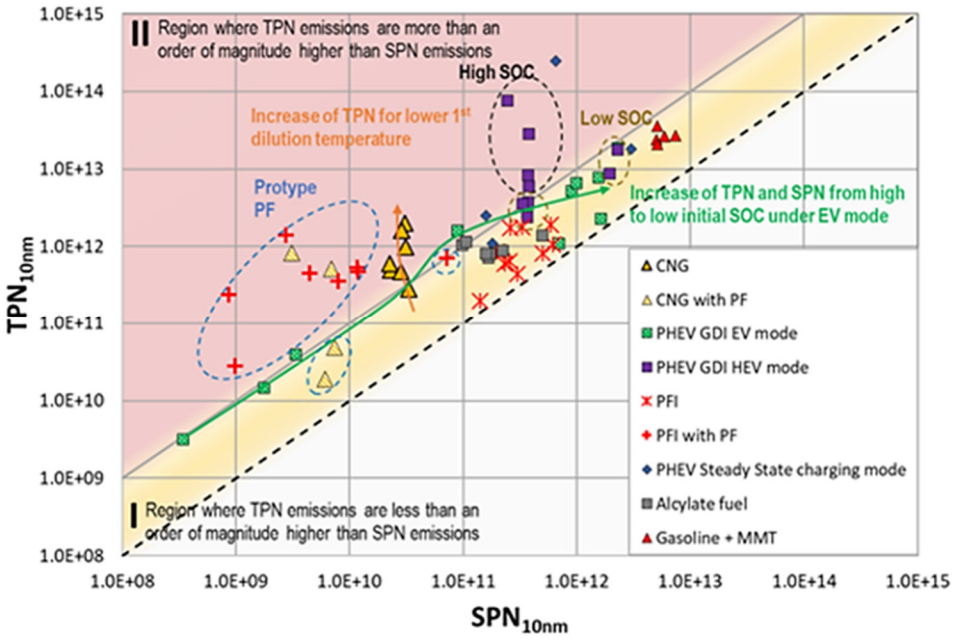


*Figure 17. Total particle number emissions from various technologies*

### *5.2. PEMs4Nano results*

The sub-23 nm laboratory and PEMS system were correlated during several testing campaigns with each other and with conventional 23 nm systems. Several equipment configurations on gasoline vehicles with and without a GPF were investigated. The developed prototypes were tested under realistic conditions on two vehicles (Vehicle 1: 1.0L GDI with GPF, EU6d-temp; Vehicle 2: 1.4L GDI without GPF, EU6b) on the chassis dynamometer using the following driving cycles:

- The Worldwide Harmonized Light Vehicles Test Cycle (WLTC).
- The US06 Supplemental Federal Test Procedure in combination with Artemis 130, selected as representative of aggressive, high-speed and high acceleration driving behaviour and rapid speed fluctuations.

In the emissions test cell, two different configurations of the equipment (A and B) were applied:

- Configuration A: the sample probes of each laboratory system (23 and 10 nm) were connected separately at the CVS tunnel, and the PEMS devices (23 and 10 nm) were connected at tailpipe (pitot tube) in the same sample location with a Y-split.
- Configuration B: the laboratory systems and the PEMS devices were both connected to the CVS tunnel (on-board systems were connected at the same location with a Y-split and the stationary systems in the same location as were in configuration A).

Various repetitions of the different cycles were performed with the two configurations.

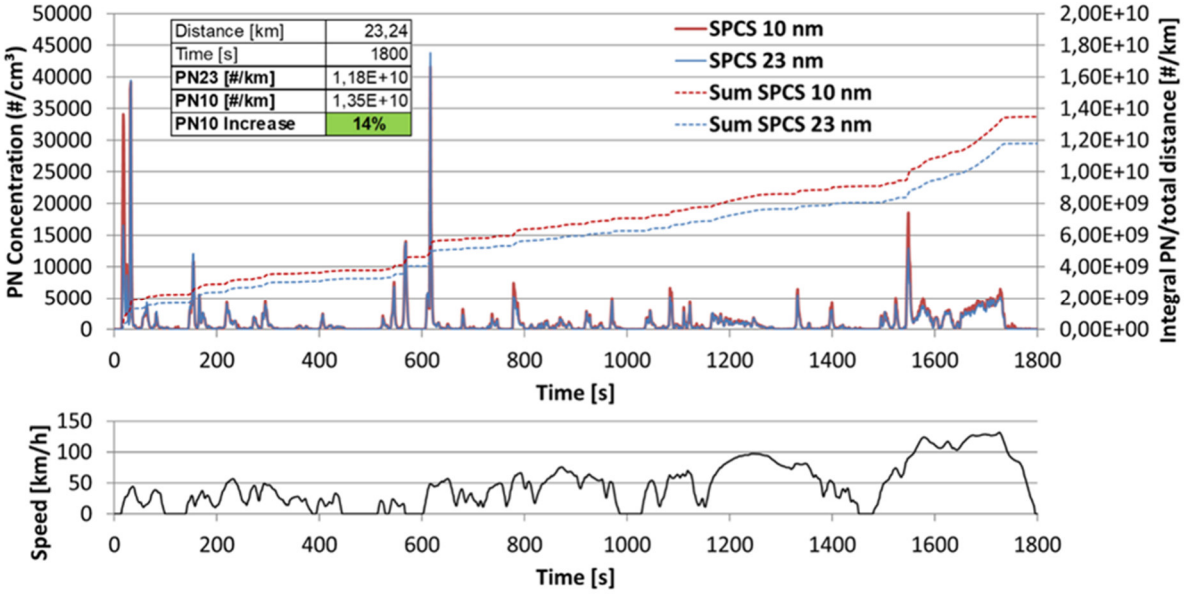


*Figure 18. WLTC test cycle PN results with 1.0L GDI with a gasoline particle filter (GPF) comparison of SPCS.*

An example of the WLTC test results of configuration A on vehicle 1, equipped with a GPF, is shown in Figure 18, where the total PN count with the 10 nm SPCS is 14% higher than the 23 nm SPCS. Furthermore, looking at the second-by-second particles concentration measurement during the cycle, sub-23 nm particles were mainly generated at engine start and acceleration phases. This trend has been shown in all different WLTP test repetitions performed in both vehicles.

Regarding the total particle number values of the three WLTP tests performed with configuration A, Figure 19 represents the average values obtained with the four different devices used.

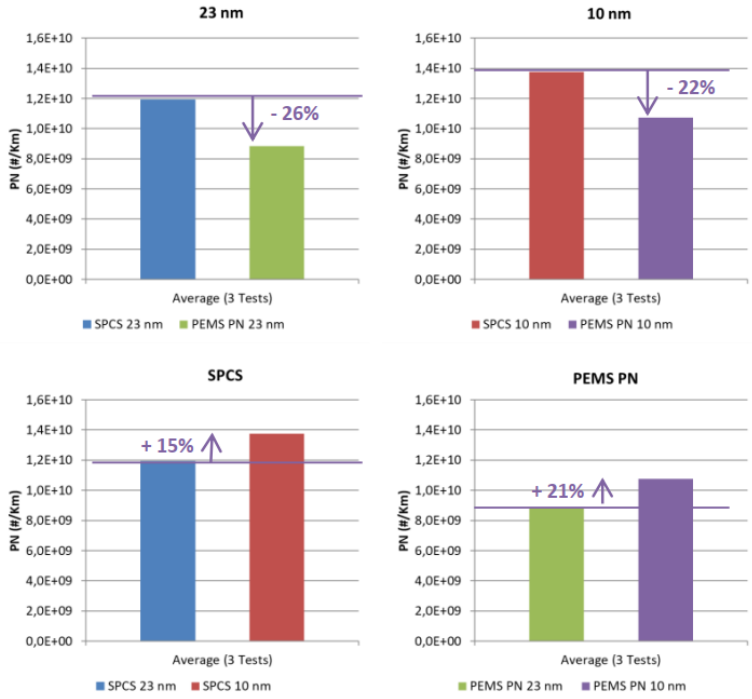


*Figure 19. Comparison between PN10 vs PN23 equipment – Average WLTC, Vehicle 1, Config. A*

Comparing the PN23 and PN10 equipment, it can be concluded that:

- More particles with SPCS are detected rather than PEMS device, both for 23 and 10 nm technology. Nevertheless, the correlation between equipment is well below the 50% limit stated in the current legislation.
- There is an increase of 15% to 21% in the total particles number by measuring with PEMs4Nano systems (PN10) compared to standard PN23 nm devices for SPCS and PEMS technologies, respectively. So, the same trend was observed in these two technologies. These results were expected due to the increase of particle size range measured.

Regarding the tests performed with the configuration B mentioned in this section, the main conclusion was that the correlation between SPCS and PEMS equipment improves once both systems are connected to the CVS tunnel at a very close sample location (from 22% to 8% in the case of PN10 and from 26% to 23% in the case of PN23nm).

The following parameters play a role in the difference in correlation between the on-board and laboratory devices:

- The measurement position: as already explained, the correlation is affected if the devices are not connected at the same sampling point.
- The Y-Split and sample probe at the pitot-tube sampling position: in order to eliminate the effect of the measurement position, a Y-split tube for the tailpipe measurement with the on-board systems (23 and 10 nm devices) was used. However, this tool may have caused some particle losses by adding more pieces in the sample setup, even though both devices had the same air flow rate.
- The calibration procedures of the systems: the different calibration procedure for each technology may have influenced the particle results.

In conclusion, for the two vehicles measured and evaluated in PEMs4Nano similar trends in terms of particles behaviour were observed with the different configurations of the aftertreatment system, one with GPF equipped and one without particle filter in the system.

### *5.3. SUREAL-23 results*

An example from SUREAL-23 measurements is given in Figure 20. The results refer to an AUDI A4, Euro 6b vehicle with mixed fuel injection (PFI and GDI) (Zinola et al., 2019). The vehicle was tested according to the RTS95 cycle. The ICAD was connected to the tailpipe via the SUREAL-23 dilution system (2-stage diluter with CS). For the PMP/CVS protocol, a CPC with a cut-off of 23 nm was used. With the ICAD, the high Sulphur content increases emissions by 7 % while for the full-SAPS oil, the emissions are multiplied by 1.7. For the CPC 23 sampling from the CVS/PMP system, even though it does not account for <23nm particles, emissions are significantly increased probably due to artefacts.

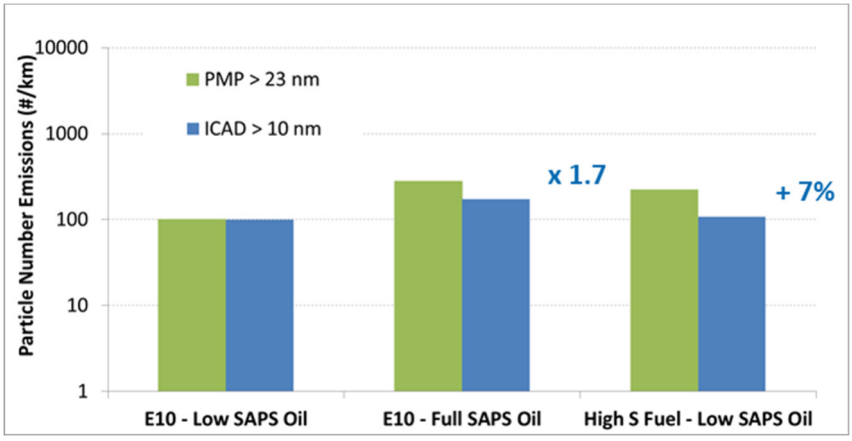


*Figure 20: CVS/PMP (ET is installed) normalised particle emissions versus tailpipe measurements with SUREAL-23 dilution system (CS is installed).*

Another example from SUREAL-23 tests is shown in Figure 21. An Alfa Romeo Giulietta, Euro 6b GDI vehicle retrofitted with a GPF was tested under the WLTC cycle. The PMP/CVS protocol used a CPC with a cut-off of 23 nm again. All other instruments shown measured from the tailpipe via the SUREAL-23 dilution system. In the graph, only the cold start phase of the WLTC is shown; the first 300 s. The instruments are in excellent agreement during the cycle. However, there were incidents where the CPC23, sampling from the CVS, fails to follow the trend imposed by the rest of the instruments, which measure from the tailpipe. These incidents are marked with the dotted circles. This delay for the CPC23 can be attributed to the CVS, which can affect the dynamic behaviour of the emissions.

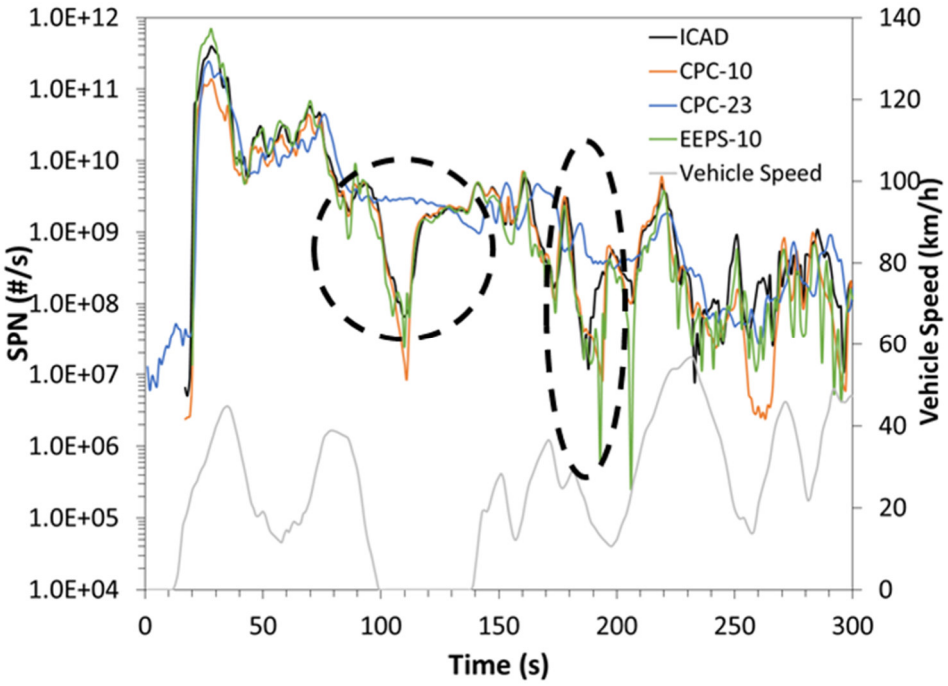


*Figure 21. Multi-instrument measurement during the first 300 s of the WLTC. CPC-23 is connected to the PMP/CVS while all other instruments are connected to the tailpipe with the SUREAL-23 dilution system. EEPS=Engine Exhaust Particle Sizer.*

Figure 22 presents results from three vehicles tested within SUREAL-23 at the same chassis dyno facility using multiple measurement instruments and multiple particle sampling and treatment methods. The graph is focused on the comparison between the PMP/CVS method using a CPC with a cut-off of 23 nm and tailpipe measurements via the ICAD. The ICAD is sampling either through the SUREAL-23 dilution system or raw. Three vehicles have been tested under "cold" or "hot" WLTC. The GDI vehicle was retrofitted with a GPF. The CNG vehicle was equipped with only a 3-way catalyst while the Diesel vehicle had a DOC, an SCR-on-filter (SCRoF) and an underfloor SCR with a clean-up catalyst. All vehicles irrespectively to the measurement methodology proved to respect Euro 6d limit. "Cold" cycle emissions are always higher than "hot" cycle emissions with the difference being more profound in the Diesel case. The GDI (retrofitted with the GPF) and the CNG vehicle (without GPF) emit nearly the same amount of >10 nm particles according to the ICAD. For the GDI, the PMP measurements are very close to the tailpipe measurements. According to EEPS results (not presented in the graph), the sub-23 nm particles fraction was minimal (4 % for the cold cycle) and 18 % for the hot one) because of the GPF. However, for the CNG, the sub-23 nm particle fraction was 42 and 31 % for the cold and hot cycle, respectively. Therefore, it can be assumed that the difference between the PMP and tailpipe measurements is because the PMP method, with the CPC23nm, does not account for sub-23 nm particles as is the case for the ICAD in the tailpipe.

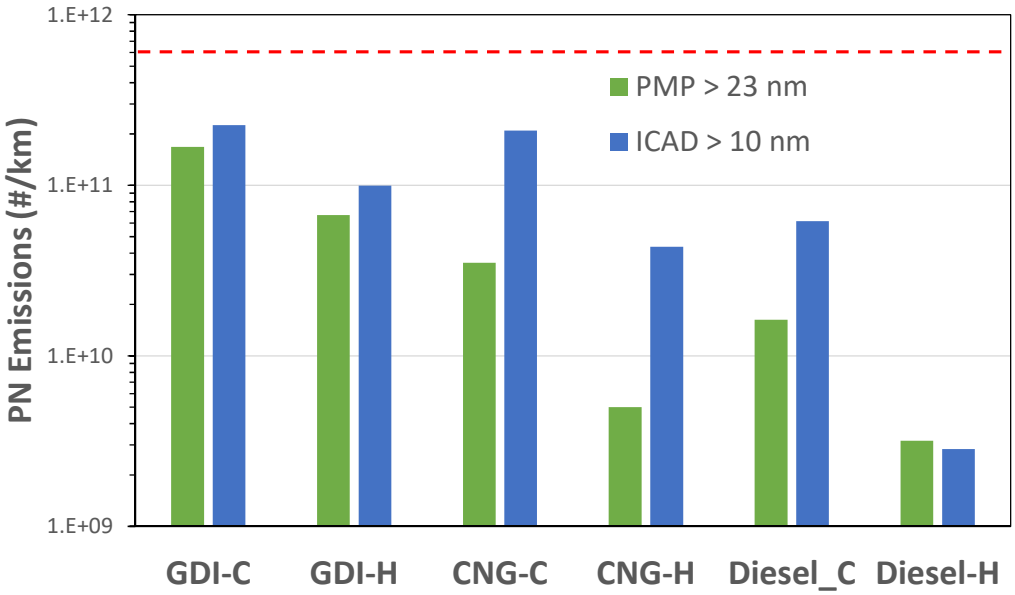


*Figure 22. Particle number emissions for three vehicles under cold (C) and hot (H) WLTC. The graph compares the PMP/CVS measurements performed with a CPC23nm to the tailpipe measurements performed with the ICAD through SUREAL-23 dilution system or raw exhaust.*

# 6. On-road measurements

## *6.1. DownToTen*

A 2000cm³ Euro 6d-temp diesel passenger car was used for on-road measurements with the DownToTen portable system. Figure 23 (urban and rural part only) and Figure 24 **(**the motorway section) show the second by second data of a representative RDE trip.

Table 2 contains the average SPN emission values for driven trips. The results are reasonable in terms of absolute SPN levels, although the average cycle results of the DownToTen system are lower than those of the commercially available PEMS.Possible reasons for this are the different PN measurement systems used in the systems (PEMS uses Diffusion Charger, DC, DTT uses CPC) and that the CPCs are designed for laboratory rather than on-road measurements.

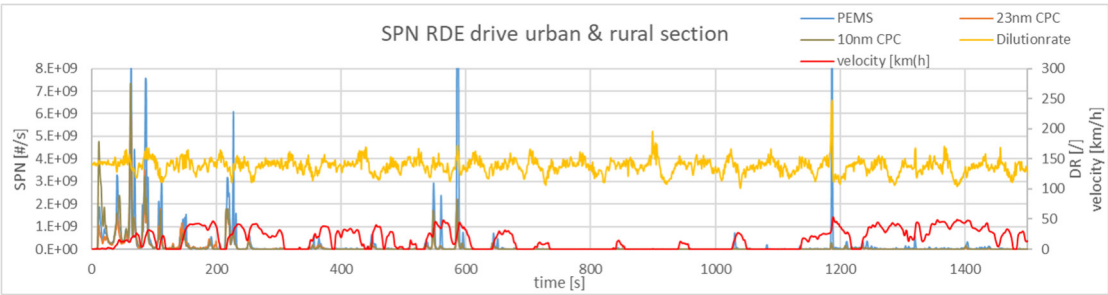


*Figure 23. Instantaneous SPN emissions and dilution rate of a RDE trip (urban and rural part only). The DownToTen measurement values are not corrected for losses.*

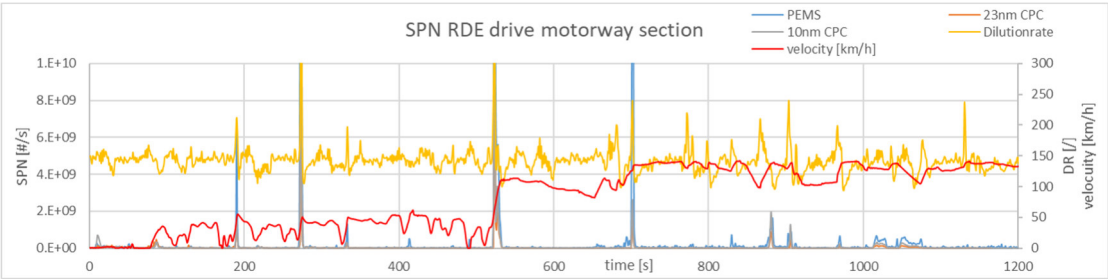


*Figure 24. Instantaneous SPN emission, dilution rate and vehicle velocity of a RDE trip (motorway part only). The DownToTen measurement values are not corrected for losses.*

*Table 2. Average SPN emissions of a RDE trip urban and rural part only (top); Average SPN emissions of a RDE trip motorway part only (bottom)*

| Average SPN values [#/km] (Urban and rural) | | |
|---|---|---|
| PEMS_23nm | DTT_PEPS_23nm | DTT_PEPS_10nm |
| 4.51E+10 | 1.95E+10 | 2.42E+10 |
| **Average SPN values [#/km] (Motorway)** | | |
| PEMS_23nm | DTT_PEPS_23nm | DTT_PEPS_10nm |
| 1.07E+10 | 2.81E+09 | 3.70E+09 |

In full throttle high speed sections on the motorway, there are peaks in the dilution ratio and also SPN peaks. Moreover, SPN peaks occur during cold start at the beginning of the RDE trip. Similar

behaviour is also recorded with a state of the art commercial PEMS, which was also mounted on the car for comparison.

In order to enable the comparison of the RDE results with the WLTC measurement results, the ERMES and a Real World Cycle (RWC) chassis dyno tests were used, cycles characterized by higher driving dynamics. Figure 25 gives an overview of SPN RDE (RDE style) emissions compared to the WLTC. For the Euro 6 CNG, direct injection car and the Euro 6 gasoline car, the WLTC measurements values are compared to a whole RDE drive, performed on a chassis dyno without road gradient. The results are as expected, SPN emission of RDE or RDE style cycles are higher than the WLTC measurement results. Exception is a Euro 6b petrol TGI vehicle, for which a WLTC cold start has been compared with an ERMES hot start and the cold start emissions outweigh the generally higher emissions in the ERMES cycle. The higher RDE or RDE style PN emissions are generally associated with the higher average cycle speed, the higher $vxa_{pos}$ and also different driven engine operating points.

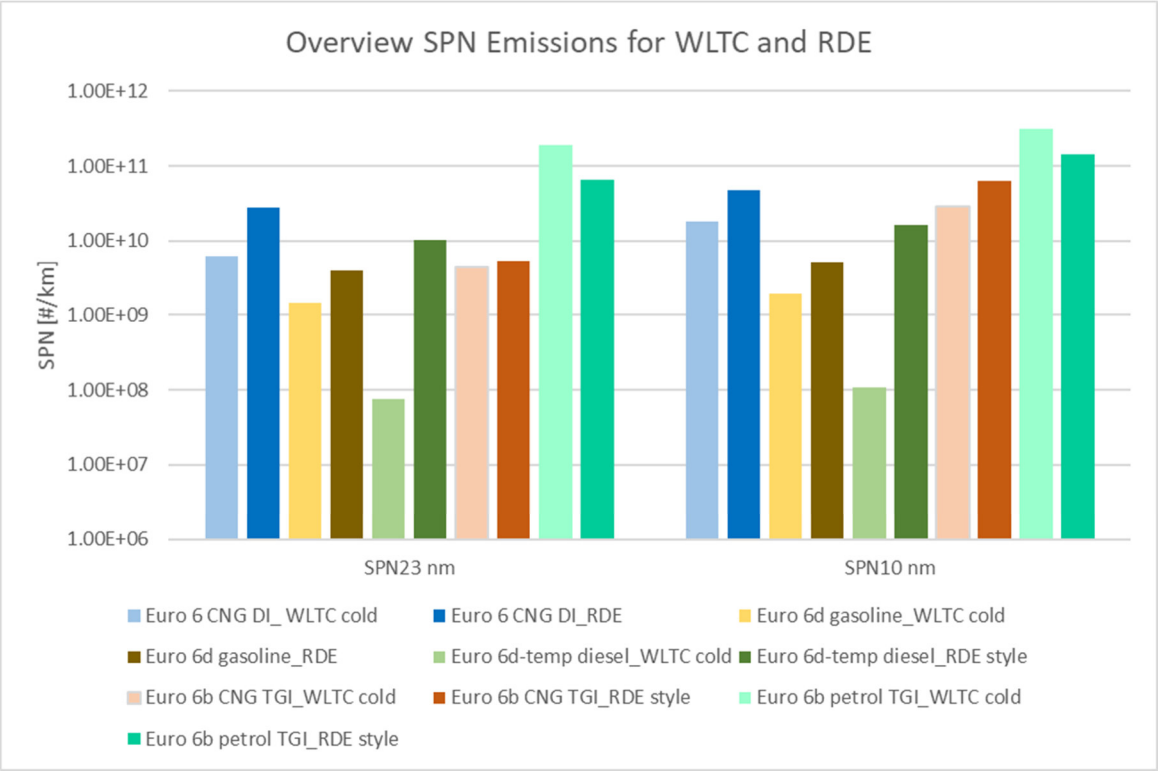


*Figure 25. Overview of SPN23 and SPN10 emission levels for WLTC and RDE. RDE style cycles refer to ERMES and RWC.*

### *6.2. PEMs4NANO*

The same two vehicles that were tested for the PEMs4NANO laboratory measurements, a 1.0 GDI vehicle equipped with a gasoline particle filter (Euro 6d-Temp) and a 1.4L GDI vehicle without GPF (Euro 6b), were also tested on real road in a third configuration (C). In the on-road equipment setup, the PN23 and the PN10 nm systems were connected at the tailpipe through a specific pitot tube according to the RDE tests standard procedures. In addition, the devices were installed at the same sample point with a Y-split.

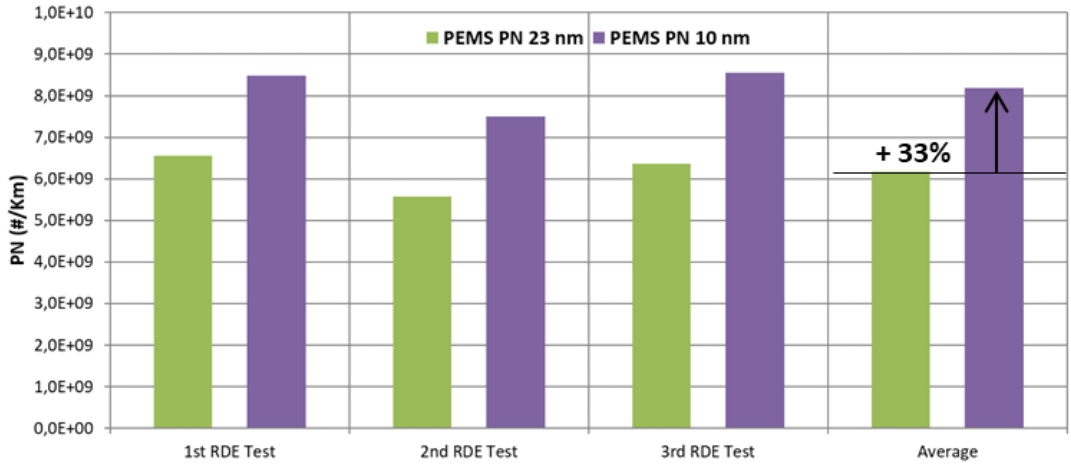


*Figure 26. Individual and average PN results of RDE Cycle – Vehicle 1 (1.0L GDI with GPF, EU6d-temp).*

The results of vehicle 1 are displayed in Figure 26 and show that the reading of the PN10 device is on average, 33% higher than the standard PN23 nm device. In addition, although there could be different conditions between each repetition of the RDE Cycle (traffic, weather, etc.) on the same route, the repeatability and consistency of the results are considered very good. The same conclusion has been observed for vehicle 2 (without GPF), for which the average PN10 measurements increase was 26%.

Figure 27 shows the PEMS PN23 and PN 10 nm second-by-second data of the 3$^{rd}$ RDE test performed at IDIADA. The main sub-23 nm particles generation events were produced during the cold engine start (first 200 seconds, see Figure 28) and different aggressive acceleration phases of the cycle.

Furthermore, looking deeper in the chart, the gap between the particles measured for each equipment increases during the motorway part of the cycle (starting from around second 3000 onwards). In the first two parts, urban and rural, the differences between measurements are due to the cold start engine and acceleration spikes, while in the last part, as mentioned, there is a progressive increase throughout the cycle. Hence, high vehicle speeds, as well as high engine loads, could lead to an increase in the particles measured by the PEMS PN10 nm compared to the PEMS PN23 nm. Nevertheless, a further and deeper investigation should be performed for a more concise explanation on this topic.

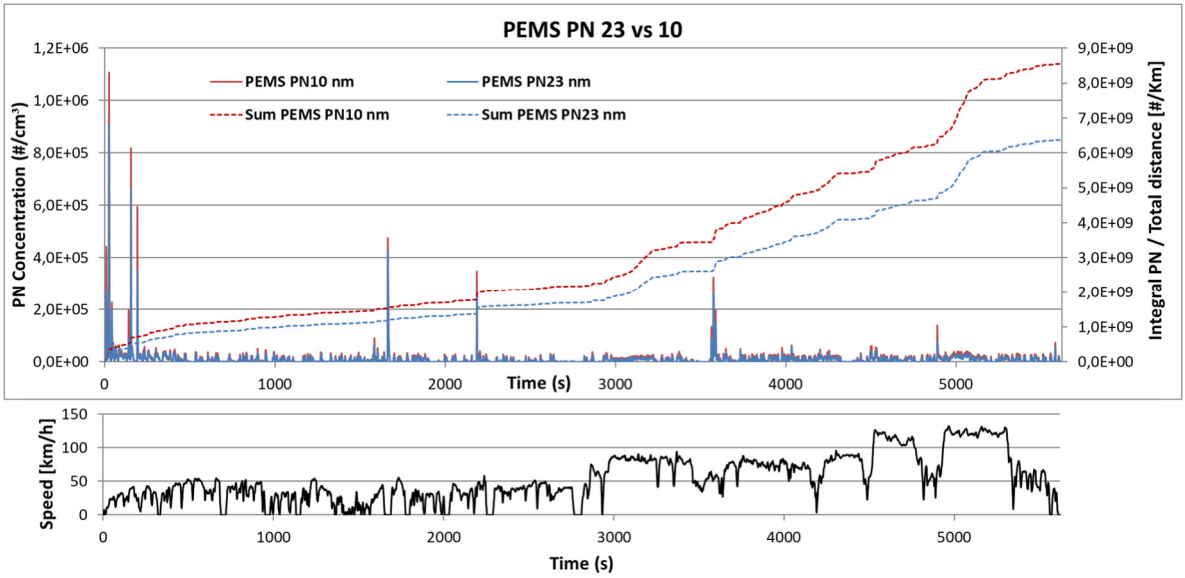


*Figure 27. Second-by-second data of the PEMS PN23 and PEMS PN10 nm systems – RDE Cycle test, vehicle 1.*

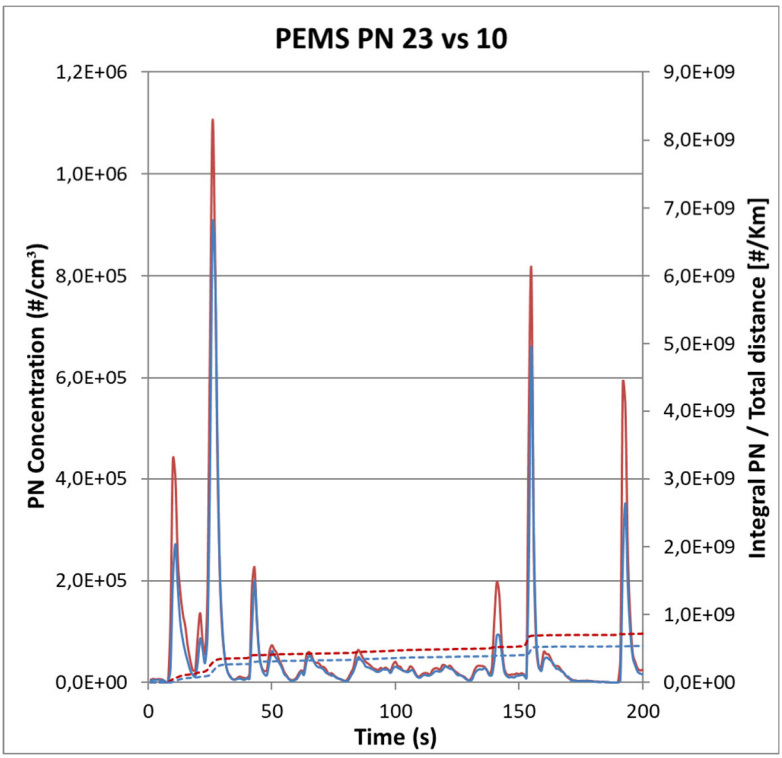


*Figure 28. Continuous PN measurement – the 200 initial seconds of the RDE cycle, , red=PEMS PN10, blue PEMS PN23.*

To sum up, a complete analysis from the different tests, configurations and vehicles has been used to define specific testing protocols to ensure the correct operation methodology for measuring small particles from 10 nm onwards at the tailpipe with the developed on-board system. In this respect, it is essential to note that in terms of measurement procedures, the equipment can be handled and applied as an existing PEMS PN23 equipment.

### *6.3. SUREAL-23*

SUREAL-23 used the ICAD for the PEMS measurements. In total, five vehicles were tested. The description of the vehicles is shown in Table 3. Two GDIs with GPFs, a hybrid GDI with GPF, a Euro6b GDI/PFI (mixed injection) without GPF and a CNG vehicle from the GASON EU project (prototype engine) have been tested. For all vehicles except the Audi Euro 6b, the ICAD was sampling directly for the raw exhaust without any dilution stage. In the case of the Audi, a passive single-stage hot dilution system was installed. No VPR was used since the ICAD can measure at elevated temperatures (up to 180 °C).

*Table 3 Vehicle characteristics tested with the ICAD on the RDE cycles*

| **Model** | **Renault Kadjar** | **Alfa Romeo Giulietta** | **Kia Niro Hybrid** | **Audi A4** | **Fiat 500L** |
|---|---|---|---|---|---|
| **Engine Capacity (l)** | 1.3 | 1.8 | 1.6 | 2.0 | 1.0l, 3-cyl |
| **Fuel** | Gasoline | Gasoline | Gasoline | Gasoline | CNG (methane) |
| **Fuel Injection** | DI | DI | DI | DI + PFI | DI |
| **GPF** | Yes | Yes | Yes | No | No |
| **Euro emissions classification** | 6d-temp | 6b with GPF retrofitted | 6d-temp | 6b | R&D, GasOn EU project |
| **Odometer (km)** | 2520 | 17550 | 7590 | 15000 | 15900 |

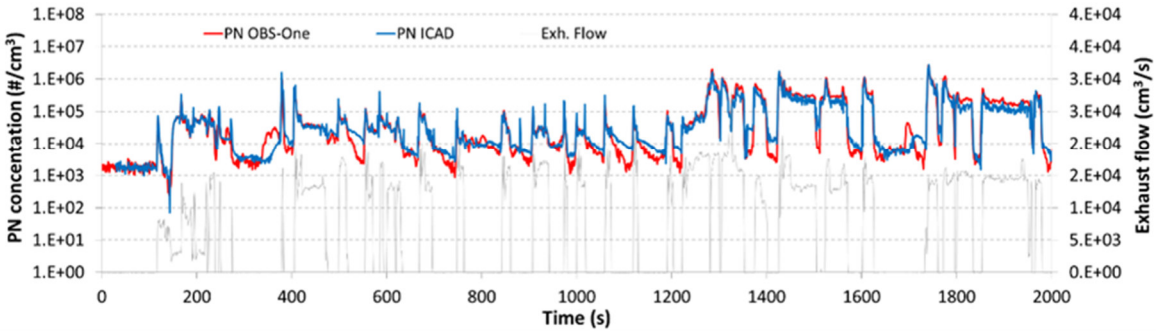


*Figure 29. Comparison of the SUREAL-23 PEMS system with the HORIBA commercial PN OBS-1 system. The vehicle shown is the hybrid one.*

For comparison, the commercial PEMS Horiba OBS-ONE was used in every case. It has to be noticed that the two particles counting instruments, the ICAD and the Horiba, have different cut-off diameters (ICAD: d50=10nm and Horiba: d50=23nm). In general, good agreement between the two instruments was observed as is depicted in Figure 29.

The summary of the results is shown in Figure 30. All vehicles respect the emission limits of their Euro class. There is a relatively good agreement between the two systems except for the CNG

case. However, this is easily explained as the CNG vehicle emits a large sub-23 nm particle fraction which is not taken into account by the commercial PEMS. The cleanest vehicles are the GDI with the company's GPF and the CNG one. The GDI Euro 6b retrofitted with a GPF also demonstrates very low emissions well below the Euro 6d-temp limit. The hybrid vehicle, although also equipped with a GPF, shows significantly higher emissions compared to the conventional GDIs; >4x from the Renault Kajar and >2x from the Alfa Romeo. In the hybrid case the increased emissions can be explained by the lower operating temperature of the engine. Finally, the advanced fuel injection technology of the Audi A4 (mixed GDI/PFI operation) results in much decreased PN emissions compared to the EURO-6b limits. It enables the marginal attainment of Euro 6d limit. The above results verify the capability of the SUREAL-23 PEMS system for on-road measurements while maintaining the significant advantages of minimal particle dilution and treatment requirements.

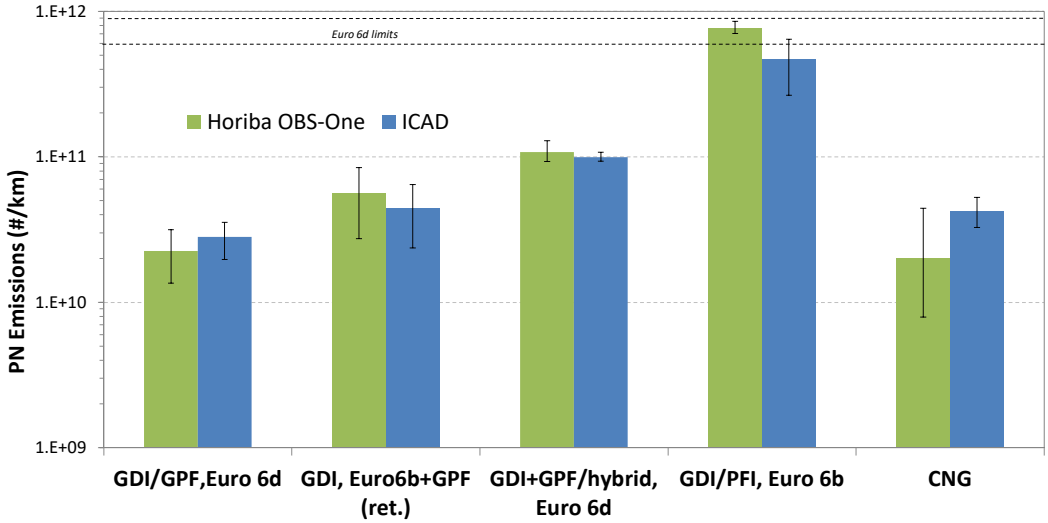


*Figure 30. SUREAL-23 on-road tests for five vehicles. The ICAD measurements are compared to the commercially available Horiba OBS-1 system.*

# 7. Conclusion and Policy Implications

## *7.1. General*

The three projects funded under the GV-02-2016 Horizon 2020 Call, supported the understanding, measurement and regulation of particle emissions below 23 nm and have successfully developed solid sub-23 nm particle measurement devices, specifically laboratory systems and mobile devices for RDE tests. The new technology was validated in chassis dyno tests and on the real road. The results show that sub-23 nm particles are mainly generated at the engine start and during acceleration phases. The innovations show that the technology is mature and robust enough to serve as a basis for regulating sub-23 nm particles. Consistently across the three projects, the catalytic stripper has been identified as a crucial component to measure solid sub-23 nm particles reliably. The CS can be designed to have both a high catalytic function efficiency and low particle losses. The project-specific conclusions and recommendations are the following.

## *7.2. DownToTen*

DownToTen has developed laboratory and portable versions of a novel sampling and measurement system, which can measure both solid and total particle numbers. The system offers a reasonable penetration efficiency for primary particles and — within normal operation — a reasonably stable DR (100±10). When the CS is in-line, the system is expected to be artefact free. Going down to lower than 10 nm particles increases both the probability of gas-to-particle artefacts and diffusion losses (penetration 40-60%). The system was used in several laboratories to assess the effects of vehicle technologies, fuels, regulatory cycles, temperatures, operating conditions and aftertreatment systems on the particle emissions.

Most vehicle technologies were found to be below the $6x10^{11}$ #/km PN23 limit value for both >23 nm and >10 nm particles. For moderate power drive cycles, emissions of vehicles with particle filters are always well below the limit value. Improvement in current filter applications will be required to bring PN10 emissions below the limit, which has been defined for solid 23 nm, with a suitable engineering safety margin in particular during severe operating conditions. This is also expected to bring PN<10 below the limit value. The highest emissions were observed from PFI passenger cars, motorcycles and mopeds, currently not subject to PN legislation. Technology improvements (including particle filters) are required to meet the current limit for PN10. Average PN emissions from gasoline hybrids in ICE mode under severing conditions may also require a GPF even for PN23.

In specific cases the vehicles emitted a significant number of particles smaller than 23 nm:

- During active Diesel PF regenerations PN emissions can be dominated by PN<10 for short periods.
- GDI vehicles may emit <23 nm soot particles under very high load transients; these particles seem to mostly fall above the PN10 threshold rather than below 10 nm.
- CNG vehicle emissions were found to be significantly elevated below 10 nm. A simple retrofit of a GPF has been seen to reduce both PN10 and PN<10 to well below the limit value. A prototype CNG operating on in-cylinder injection exhibited PN<23/PN23 ratios that were below 2.5 times.
- In RDE measurements, the measured PN10 and PN23 emissions are influenced by the soot loading both in diesel and gasoline filter applications. Higher PN emissions are detected after regeneration. PN10 and PN23 emission levels over RDE are usually above the WLTP levels.
- Total Particle Number (TPN) emissions also seem lower than levels measured for corresponding combustion technologies one decade ago. This could be an indication that emission control technologies introduced for hydrocarbons and solid particle control also led to reductions in total particle number. Specific GDI operation events, such as high

accelerations and steady-state high speeds, can increase emissions of such particles, to levels more than an order of magnitude higher than SPN emissions.

Based on these observations, the areas that are identified for further development are (1) improvements in filtration efficiency of GPFs and particle filters for gas engines (2) development of optimal DPF regeneration strategies that maintain the minimum soot cake for high filtration efficiency, (3) raw vs dilute sampling, (4) Total Particle Number measurement, (5) development of robust calibration procedures for PN10 - with a view to PN<10, gas engine particle emissions, (6) ultra-clean combustion and fuel combinations beyond CNG and (7) ultra-low ash fuels and lubricants.

### *7.3. PEMs4Nano*

The measurement device achieved a detection efficiency at 10 nm of 20%. The catalytic stripper was optimised to have >60% penetration efficiency at a particle size of 8 nm, and a removal efficiency of the semi-volatiles of >99% for tetracontane particles. The new technology was tested and correlated using chassis dyno tests and real road tests. The repeatability of the devices is within the current legislative limit, and the new sub-23nm lab and on-board systems can be applied and handled as the established PN23 measurement systems.

The results show that sub-23 nm particles are mainly generated at the engine start and during acceleration phases. Multitechnique analysis shows that (1) the smallest nanoparticles have the most important surface-organic fraction, and (2) the highest stripping efficiency of the CS is recorded on the smallest nanoparticles. The penetration of solid particles can be maximised while semi-volatile materials can be removed such that semi-volatile particles are eliminated from the exit stream for the catalytic stripper. Measurement of semi-volatile particle number in addition to solid particle number remains problematic, as number concentration and size remain highly variable and influenced by dilution rates and temperatures.

The combination of model guided application (MGA), advanced measurement technologies and procedures open the door to optimising and developing engine technologies and aftertreatment systems faster and at lower costs. During the design phase, MGA offers an improved understanding of particle characteristics. During the testing phase, it can be used to identify optimal sampling positions in the exhaust line and at the tailpipe. The workflow supports the decision-making process to further reduce PN emissions, for example, by optimising fuel injection equipment (FIE), fuel composition and sampling conditions.

### *7.4. SUREAL-23*

Within SUREAL-23 significant breakthroughs have been realised in instrumentation and methodology. Both the ICAD and the HM-DMA are capable of hot measurements, thereby eliminating a large part of the necessary but complex PMP-conformant dilution system. In addition, SUREAL-23 developed an advanced dilution system, consisting of a typical two-stage diluter and the Volatile Particle Remover (VPR). The innovative ejector-type dilution system uses a Catalytic Stripper (CS) for the VPR function, demonstrating minimal particle losses and measurement artefacts for the sub-23 nm particle size area and excellent volatiles and sulphur removal efficiency.

For measuring sub-23 nm solid particles, a highly efficient volatile removing system is necessary. During the project, it was demonstrated that conventional Evaporation Tube (ET) technology is not sufficient to remove volatile particles in this particle size range effectively. On top of that, it creates artefacts. Within SUREAL-23, the developed CS was very effective in volatiles removal while at the same time demonstrating minimal sub-23 nm particle losses. Moreover, the size-dependency of the minor particle losses were very well characterised.

SUREAL-23 examined the effect of particular conditions (specific fuels, fuel additives, lubricants, ethanol or RME content levels, etc.) on the sub-23 nm exhaust particle number concentration and

volatile content. During the project, Diesel, GDI, GDI/PFI, hybrid and NG vehicles were examined. Each technology has been assessed according to several different measurement methodologies. As such, the project offered the possibility to evaluate those measurement methodologies and instruments under various conditions. SUREAL-23 sampling and measurement instruments enabled reliable measurements from the exhaust tailpipe. The tailpipe method proved to be superior to the typical CVS-based method, especially when sub-23 nm particles are also included. The project's PEMS was also used very successfully for RDE measurements. The latter provided equivalent to laboratory test results when the SUREAL-23 instrumentation was used.

In general, SUREAL-23 reaffirmed that there could be high concentrations of exhaust particles in size range below 23 nm. Most of them are volatile, but there is a significant fraction of non-volatiles (metals, soot, salts, etc.).

For diesel engines:

- Most diesel vehicles are equipped with very efficient DPF's (eff. >99%). These filters, as long as they work properly, remove smaller (sub 23nm) particles even more efficiently due to the Brownian diffusion filtration mechanism.

For SI engines:

- GDI engines emit high concentrations of particles in the range of 10 to 40 nm. Still, the smallest particles will also be removed efficiently for vehicles equipped with the latest state-of-the-art GPFs (at least as efficient as DPFs). If the regulation takes into account 10-23 nm particles, this will ensure the installation of the most efficient filters.

    - In SUREAL-23 the PFI and CNG vehicles examined were not emitting above the 6x1011 #/km limit even for the SPN10nm. However, it was demonstrated that the oil type and the increased lube oil consumption might lead to significantly higher emissions; therefore, PFI and CNG should be included in the regulation.

- 

### *7.5. European Commission*

Based on the above conclusions and recommendations, the European Commission is taking the results from theseprojects as an input to define research topics for future work programmes (both in terms of technology and air quality and health research) and shares them with relevant policy Directorates-General as feedback to policy and as a potential basis for implementing new regulations or amend existing ones for particulate matter and air quality.

## 8. Acknowledgements

The DownToTen project has received funding from the European Union's Horizon 2020 research and innovation programme under agreement No 724085.

The PEMs4Nano project has received funding from the European Union's Horizon 2020 research and innovation programme under agreement No 724145.

The SUREAL-23 project has received funding from the European Union's Horizon 2020 research and innovation programme under agreement No 724136.

## 9. Disclaimer

The opinions expressed in this manuscript are those of the authors and should in no way be considered to represent an official opinion of the European Commission. Mention of trade names or commercial products does not constitute endorsement or recommendation by the authors or the European Commission.

## 10. Conflicts of interest

The authors declare no conflict of interest.

## 11. References


Baltzopoulou, P., Melas, A., Vlachos, N., Deloglou, D., Papaioannou E., Konstandopoulos, A.G., 2019. Solid Nucleation Mode Engine Exhaust Particles Detection at High Temperatures with an Advanced Half Mini DMA. SAE Technical Paper 2019-24-0052, SAE Int. J. of Advances and Current Practices in Mobility. DOI: 10.4271/2019-24-0052

Bainschab, M., Martikainen, S., Keskinen, J., Bergmann, A., Karjalainen P., 2019. Aerosol gas exchange system (AGES) for nanoparticle sampling at elevated temperatures: Modeling and experimental characterization. Scientific Reports 9, 17149.

Burtscher, H., 1992. Measurements and Characteristics of Combustion Aerosols with Special Consideration of Photoelectric Charging and Charging by Flame Ions, J. Aerosol Sci. 23, 549-595.

Chasapidis, L., Melas, A., Tsakis, A., Zarvalis, D., Konstandopoulos, A., 2019. A Sampling and Conditioning Particle System for Solid Particle Measurements Down to 10 nm. SAE Technical Paper 2019-24-0154, https://doi.org/10.4271/2019-24-0154.

Duca, D., Irimiea, C., Faccinetto, A., Noble, J. A., Vojkovic, M., Carpentier, Y., Ortega, I. K., Pirim, C., Focsa, C., 2019. On the benefits of using multivariate analysis in mass spectrometric studies of combustion-generated aerosols. Faraday Disc. 218, 115-137 doi:10.1039/C8FD00238J.

D. Duca, M. Rahman, Y. Carpentier, C. Pirim, A. Boies, C. Focsa, 2021. Chemical characterization of size-selected nanoparticles emitted by a gasoline direct injection engine: impact of a catalytic stripper. Fuel 294, 120317. doi: 10.1016/j.fuel.2021.120317

Etheridge, J., Mosbach, S., Kraft, M., Wu, H., & Collings, N., 2011. Modelling cycle to cycle variations in an SI engine with detailed chemical kinetics. Combustion and Flame, 158, 179-188.

Faccinetto, A., Focsa, C., Desgroux, P., Ziskind M., 2015. Progress toward the Quantitative Analysis of PAHs Adsorbed on Soot by Laser Desorption/Laser Ionization/Time-of-Flight Mass Spectrometry. Environ. Sci. Technol. 49, 10510-10520.

Fernández de la Mora J., 2017. Expanded size range of high-resolution nanoDMAs by improving the sample flow injection at the aerosol inlet slit. J. of Aerosol Science, 113, 265-275.

Fernandez de la Mora, J., Perez-Lorenzo L.J., Arranz, G., Amo-Gonzalez, M., Burtscher, H., 2017. Fast high-resolution nanoDMA measurements with a 25 ms response time electrometer, Aerosol Science and Technology, 51 (6), 724-734.

Fierz, M., Meier, D., Steigmeier, P., Burtscher, H., 2014. Aerosol Measurement by Induced Currents, Aerosol Science and Technology, 48:4, 350-357, DOI: 10.1080/02786826.2013.875981

Focsa, C., Duca, D., Noble, J., Vojkovic, M., Carpentier, Y., Pirim, C., Betrancourt, C., Desgroux, P., Tritscher, T., Spielvogel, J., Rahman, M., Boies, A., Lee, K. F., Bhave, A. N., Legendre, S., Lancry, O., Kreutziger, P., Rieker, M., 2020. Multi-technique physicochemical characterization of particles

generated by a gasoline engine: towards measuring tailpipe emissions below 23 nm. Atmos. Environ. 235, 117642. doi: 10.1016/j.atmosenv.2020.117642.

Giechaskiel, B., Lähde, T., Suarez-Bertoa, R., Clairotte, M., Grigoratos, T., Zardini, A., Perujo, A., Martini, G., 2018. Particle number measurements in the European legislation and future JRC activities. Combust. Engines 174, 3–16.

Giechaskiel, B. Lähde, T., Drossinos, Y., 2019a. Regulating particle number measurements from the tailpipe of light-duty vehicles: The next step? Environmental Research 172, 1–9.

Giechaskiel, B. and Martini, G., 2014. Engine Exhaust Solid Sub-23 nm Particles: II. Feasibility Study for Particle Number Measurement Systems. SAE Int. J. Fuels Lubr. 7 1-15. doi:10.4271/2014-01-2832.

Graves, B. M., J. S. Olfert, B. Patychuk, R. Dastanpour, S. N. Rogak, 2015. Characterization of Particulate Matter Morphology and Volatility from a Compression-Ignition Natural-Gas Direct-Injection Engine. Aerosol Science and Technology 49, 589–98. doi: 10.1080/02786826.2015.1050482.

Irimiea, C., Faccinetto, A., Mercier, X., Ortega, I. K., Nuns, N., Therssen. E., Desgroux, P., Focsa, C., 2019. Unveiling trends in soot nucleation and growth: When secondary ion mass spectrometry meets statistical analysis. Carbon 144, 815-830. doi:10.1016/j.carbon.2018.12.015.

Kazemimanesh, M., M. Rahman, D.Duca, T. J. Johnson, A. Adad, G. Giannopoulos, C. Focsa, A. M. Boies, 2021. Morphology and volatility of particulate emissions from gasoline direct injection engine using aerodynamic diameter, mobility diameter, and mass measurements in tandem. *Journal of Aerosol Science* Under review.

Kumar P., Robins A., Vardoulakis S., Britter R., 2010. A review of the characteristics of nanoparticles in the urban atmosphere and the prospects for developing regulatory controls. Atmos. Environ. 44, 5035–5052.

Lee, K., Eaves, N., Mosbach, S., Ooi, D., Lai, J., Bhave, A., Manz, A., Geiler, J.N., Noble, J.A., Duca, D., Focsa C., 2019. Model Guided Application for Investigating Particle Number (PN) Emissions in GDI Spark Ignition Engines. SAE Int. J. Adv. & Curr. Prac. in Mobility 1, 76-88.

Melas, A.D., Koidi, V., Deloglou, D., Daskalos,E., Zarvalis, D., Papaioannou, E. & Konstandopoulos, A.G., 2020. Development and evaluation of a catalytic stripper for the measurement of solid ultrafine particle emissions from internal combustion engines. Aerosol Science and Technology, 54, 6, 704-717.

Momenimovahed, A., Olfert, J. S., 2015. Effective Density and Volatility of Particles Emitted from Gasoline Direct Injection Vehicles and Implications for Particle Mass Measurement. *Aerosol Science and Technology* 49. 1051–62. doi: 10.1080/02786826.2015.1094181.

Ngo, L. D., Duca, D., Carpentier, Y., Noble, J. A., Ikhenazene, R., Vojkovic, M., Irimiea, C., Ortega, I. K., Lefevre, G., Yon, J., Faccinetto, A., Therssen, E., Ziskind, M., Chazallon, B., Pirim, C., Focsa, C., 2020. Chemical discrimination of the particulate and gas phases of miniCAST exhausts using a two-filter collection method, Atmos. Meas. Tech. 13, 951-967

Ortega, A., Marques, F., Tsakalidis, A., Kousoulidou, M., Gkoumas, K., Grosso, M., Pekar, F., 2020. Research and innovation in road vehicle emissions control: An assessment based on the Transport Research and Innovation Monitoring and Information System (TRIMIS) to support the development of future European pollutant emission standards, European Commission, ISBN 978-92-76-19431-6

Popovicheva, O. Irimiea, C., Carpentier, Y. , Ortega, I. K., Kireeva, E., Shonija, N., Schwarz, J., Vojtisek, M., Focsa, C., 2017. Chemical Composition of Diesel/Biodiesel Particulate Exhaust by FTIR Spectroscopy and Mass Spectrometry: Impact of Fuel and Driving Cycle. Aerosol Air Qual. Res. 17, 1717-1734

Ristimäki, J., K. Vaaraslahti, M. Lappi, and J. Keskinen, 2007. Hydrocarbon Condensation in Heavy-Duty Diesel Exhaust. *Environmental Science & Technology* 41, 6397–6402. doi: 10.1021/es0624319.

Sakurai, H., 2007. Primary Standard for Aerosol Particle Number Concentration. Presented at the 11th ETH Conference on Combustion Generated Nanoparticles, Zurich, Switzerland, August 13–15, 2007.

Sakurai, H., Tobias, H. J., Park, K., Zarling, D., Docherty, K. S., Kittelson, D. B., McMurry, P. H., Ziemann, P. J., 2003. On-line measurements of diesel nanoparticle composition and volatility. *Atmospheric Environment* 37, 1199–1210. doi: 10.1016/S1352-2310(02)01017-8.

Samaras, Z.C., Andersson, J., Bergmann, A., Hausberger, S., Toumasatos, Z., Keskinen, J., Haisch, C., Kontses, A., Ntziachristos, L.D., Landl, L., Mamakos, A., Bainschab M., 2020. Measuring Automotive Exhaust Particles Down to 10 nm. SAE Technical Paper 2020-01-2209, doi:10.4271/2020-01-220

Simonen P., J. Kalliokoski, P. Karjalainen, T. Rönkkö, H. Timonen, S. Saarikoski, M. Aurelab, M. Bloss, G. Triantafyllopoulos, A. Kontses, S. Amanatidis, A. Dimaratos, Z. Samaras, J. Keskinen, M. Dal Maso, L. Ntziachristos, 2019. Characterization of laboratory and real driving emissions of individual Euro 6 light-duty vehicles – fresh particles and secondary aerosol formation *Environmental Pollution* 255, 113175 https://doi.org/10.1016/j.envpol.2019.113175

Thaler K., L. Gilardi, A. Vohburger, A. Kontses, Z. Toumasatos, Z. Samaars, J. Kalliokoski, P. Simonen, H. Timonen, M. Aurela, S. Saarikoski, S. Martikainen, P. Karjalainen, M. Dal Maso[3], J. Keskinen, R.

Niessner, G. A. Pang, Ch. Haisch, 2021. HELIOS/SICRIT/Mass Spectrometry for Analysis of Aerosols in Engine Exhaust, *Aerosol Science & Technology*, submitted

Toumasatos, Z., Kontses, A., Doulgeris, S., Samaras, Z., Ntziachristos, L., 2020. Particle emissions measurements on CNG vehicles focusing on Sub-23nm, Aerosol Science and Technology, 55, 182-193. DOI: 10.1080/02786826.2020.1830

Utry, N., Ajtai, T., Filep, Á., Pintér, M., Török, Z., Bozóki, Z., & Szabó, G., 2014. Correlations between absorption Angström exponent (AAE) of wintertime ambient urban aerosol and its physical and chemical properties. Atmospheric Environment, 91, 52–59.

http://dx.doi.org/10.1016/j.atmosenv.2014.03.047.

Yu, C., Seslija, M., Brownbridge, G., Mosbach, S., Kraft, M., Parsi, M., Bhave, A., 2020. Deep kernel learning approach to engine emissions modeling. *Data-Centric Engineering, 1*, E4. doi:10.1017/dce.2020.4

Zinola, S., Leblanc, M., Rouleau, L., Dunand, X., Baltzopoulou, P., Chasapidis, L., Deloglou, D., Melas, A.G. Konstandopoulos, A.D., Ruggeberg, T., Fierz, M., Burtscher, H., Tejero, A., Amo, M., Zamora, D., 2019. Measurement of sub-23 nm particles emitted by gasoline direct injection engine with new advanced instrumentation. JSAE 20199152, SAE Technical Paper 2019-01-2195.